DESIGN OF PHOTOVOLTAIC ENERGY SYSTEMS FOR ISOLATED COMMUNITIES

by

Abdoulaye SOW

MANUSCRIPT BASED THESIS
PRESENTED TO ÉCOLE DE TECHNOLOGIE SUPÉRIEURE IN PARTIAL FULFILLMENT FOR THE DEGREE OF MASTER IN MECHANICAL ENGINEERING
M.A.SC

MONTREAL, NOVEMBER 08 TH 2019

ÉCOLE DE TECHNOLOGIE SUPÉRIEURE
UNIVERSITÉ DU QUÉBEC

BOARD OF EXAMINERS

THIS THESIS HAS BEEN EVALUATED

BY THE FOLLOWING BOARD OF EXAMINERS

Mr. Daniel Rousse Thesis Supervisor
Professor, Mechanical engineering at École de technologie supérieure

Mr. Mathias Glaus, President of the Board of Examiners
Professor, Construction engineering at École de technologie supérieure

Didier Haillot, Member of the jury
Invited Professor, Mechanical engineering at École de technologie supérieure

THIS THESIS WAS PRENSENTED AND DEFENDED

IN THE PRESENCE OF A BOARD OF EXAMINERS AND PUBLIC

JULY 18TH 2018

AT ÉCOLE DE TECHNOLOGIE SUPÉRIEURE

ACKNOWLEDGMENT

I would first like to thank my thesis advisor Mr Daniel Rousse Professor in Mechanical engineering at École de technologie supérieure for his patience, motivation, and support. He consistently allowed this paper to be my own work but steered me in the right direction whenever he thought I needed it.

I would also like to thank the member of the t3e research group for the stimulating discussions, and for all the fun we have had in the last two years.

I would also like to acknowledge the financial support for conducting this research from FRQNT (Fonds de Recherche du Québec Nature et Technologies), MERN (Ministère de l'Énergie et des Ressources Naturelles du Québec) and from M. Michel Trottier for his generous donation to the t3e research group

Finally, I must express my very profound gratitude to my parents Ousmane and Sophie for providing me with unfailing support and continuous encouragement throughout my years of study and through the process of researching and writing this thesis. I also want to thank my brothers Thierno and Mouhamed and my sister Oumouratou for continuing motivating me and supporting me. This accomplishment would not have been possible without my family. Thank you.

CONCEPTION D'UN SYSTÈME D'APPROVISIONNEMENT ÉNERGETIQUE PHOTOVOLTAIQUE POUR COMMUNAUTÉS ISOLÉES

Abdoulaye SOW

RÉSUMÉ

L'accès à l'énergie joue un rôle important dans un processus de développement économique social et humain. Cependant, de nos jours 1,3 milliard de personnes n'ont toujours pas accès à l'électricité. La majorité de ces communautés vivent dans les zones rurales des pays sous-développés. Pour faire face à cette question, les systèmes PV décentralisés constituent des solutions appropriées pour l'électrification et le pompage de l'eau. De plus, avec la récente baisse des coûts des panneaux photovoltaïques et des batteries, des systèmes plus sophistiqués intégrant le contrôle de l'énergie produite en fonction du niveau de consommation ont été développés.

Pour soutenir cette implantation, des logiciels et outils numériques permettant un dimensionnement précis et optimal de ces systèmes ont été développés. PV SOL, PV SYST, HOMER ou iHOGA peuvent être cités comme exemples de logiciels de prédiction. Néanmoins, malgré le niveau de sophistication de ces programmes, il existe un besoin de proposer un logiciel de prédiction simple, évolutif, précis et gratuit pour permettre aux communautés isolées de calculer les systèmes dont elles ont besoin.

Ce mémoire présente un programme qui utilise un algorithme génétique pour le dimensionnement optimal d'un système PV-batteries pour électrifier les communautés hors-réseau. Le programme a été développé en Python. Il simule le comportement des systèmes PV-batteries installés dans tous les endroits où des données météorologiques sont disponibles. En outre, une banque de données modifiable, adaptable et évolutive avec le temps des différents composants du système est disponible.

Dans ce mémoire, une maison, une école, des lampadaires et un centre de santé situés à ELDORET au Kenya sont analysés comme cas d'étude. Les systèmes PV-batteries optimisés conçus par le programme ont été comparés à iHOGA et HOMER. La validation a révélé un écart maximal de 12% entre les résultats du programme et ceux de iHOGA. Ceci pouvant être alloué à une différence de modélisation.

La gratuité, l'évolutivité et la future disponibilité du programme permet d'affirmer qu'un logiciel simple sera désormais disponible pour les communautés isolées qui ne peuvent accéder aux logiciels commerciaux.

Mots clés : Décentralisé, Photovoltaïque, Dimensionnement, Optimisation, Algorithme génétique

DESIGN OF A PHOTOVOLTAIC ENERGY SUPPPLY FOR ISOLATED COMMUNITIES

Abdoulaye SOW

ABSTRACT

Access to energy has always played a significant role in economic, social, and human development. However, nowadays 1.3 billion people still do not have access to electricity. The majority of these communities live in rural areas of underdeveloped countries. To face this issue, decentralized PV systems are suitable solutions for household electrification and water pumping. In addition, with the recent drop of PV panel's and batteries cost, more sophisticated systems that integrate power management control strategies appear.

To support this implementation, different tools and programs helping a precise and optimal sizing of this system were made available. PV SOL, PV SYST, HOMER or iHOGA can be cited as example of prediction programs. Nonetheless, in spite of the level of sophistication of these different programs, a free access program allowing an accurate, precise and optimal design of PV-battery systems is still needed.

This thesis presents a program that uses genetic algorithm for the optimal sizing of PV-battery systems. The program was developed in Python. It simulates the behaviour of PV-battery systems installed in any location where meteorological data is available. The optimal number and the type of PV modules, batteries and inverters are provided as a result. In addition, an evolutive, adaptable, alterable data bank of the different components of the system is readily available.

In this thesis, a house, a school, floors lamps and a health care center for the remote community of ELDORET in Kenya are analysed as a case study. The optimal PV-Battery systems designed by the program were compared to the result of a classical sizing method and other software like iHOGA and HOMER. The validation process revealed a maximum gap of 12% between the program and iHOGA. A gap that can be attributed to a modelling difference.

The results were found to be in fair agreement with other predictions and therefore it is believe that the novel, free and adaptable program meets the need of remote communities when it comes to design optimal PV solar systems.

Keywords: Decentralized, photovoltaic, optimisation, Sizing, Genetic Algorithms

TABLE OF CONTENTS

LIST OF TABLES

LIST OF FIGURES

Page

LIST OF ABREVIATIONS

AC	Alternative Current
ACO	Ant colony Optimization
ANN	Artificial Neutral Network
AOI	Angle Of Incidence
DC	Direct Current
DOD	Depth Of Discharge
EPS	Excess of power Supply
FF	Fill Factor
GA	Genetic Algorithm
GUI	Graphical User Interface
GRI	Graphical Results Interface
HDKR	Hay, Davies, Klutcher and Reindl
HOMER	Hybrid Optimization Modelling Energy renewable
iHOGA	improved Hybrid Optimization by Genetic Algorithm
KibaM	Kinetic Battery Model
LPS	Loss of Power Supply
LPSP	Loss Of Power Supply Probability
NPV	Net Present Value
NREL	Natioanl renewable Energy Laboratory
POA	Plane Of Array
PSH	Peak Sun Hours
PSO	Particle Swarm Optimization
PV	Photovoltaique
RESCO	Renewable Energy Service Company
SHS	Solar Home System
SOC	State Of Charge
Trnsys	Transient Energy System Simulation

LIST OF SYMBOLS

Usual character

a empirically determined coefficient in the PV module model of SANDIA laboratory, [-]
altitude in the Hottel's model, [km]

A altitude in Hottel's model, [km]

$Ah_{restored}$ ampere-hours stored in the battery during the overcharging, [Ah]

A_i anisotropic index, [-]

AM_a absolute air mass in the PV module model of SANDIA laboratory, [-]

a_0 calculated coefficient of Hottel's model, [-]

a_1 calculated coefficient of Hottel's model, [-]

a_0^* calculated coefficient of Hottel's model, [-]

a_1^* calculated coefficient of Hottel's model, [-]

b empirically determined coefficient in the PV module model of SANDIA laboratory, [-]

B defined coefficient of the equation of time [-]
width of the first tank [-]

C battery capacity, [Ah] C_{Batt} unit price cost of the battery, [$US]

C_{Conv} unit price cost of the converter, [$US]

$C_{conv-bid}$ unit price cost of the bidirectional converter, [$US]

C_i initial capital cost, [$US]

C_{inv} unit price cost of the inverter, [$US]

C_{OM} present value of the operation and maintenance, [$US]

C_{PV} unit price cost of the PV module, [$US]

C_R required battery capacity to fulfill the demand, [kWh]

C_0, C_1, C_2, C_3, C_4, C_5, C_6 couple of coefficients traducing the solar irradiance influence in the PV module model of SANDIA laboratory

C_{10} battery capacity for a discharge current equal to I_{10}, [Ah]
self-discharging rate, [%]

D_{AC} daily use of AC appliance, [-]

D_{DC} daily use of DC appliance, [-]

$DoD_{\max}$ maximum depth of discharge, [%]

D_R needed day of storage, [d]

E_{AC} AC produced energy, [kWh]

$E_{bat\max}$ battery maximum energy, [kWh]

$E_{bat\min}$ battery minimum energy, [kWh]

E_{DC} DC produced energy, [kWh]
E_e effective solar irradiance in the PV module model of SANDIA, [W/m^2]
E_i measured irradiance, [W/m^2]
E_t equation of time, [-]
E_T total daily energy demand, [kWh]
f horizon brightening factor, [-]
F_{c-s} view factor from the sky to the collector, [W/m^2]
F_{c-hz} view factor from the horizon to the collector, [-]
F_{c-g} view factor from the ground to the collector, [-]
F_t ratio of the amount of charge of the two tanks
G_{on} extraterrestrial radiation incident on a plane surface, [W/m^2]
G_{SC} solar constant, [W/m^2]
H daily total irradiation, [W/m^2]
$\overline{H}$ monthly total irradiation, [W/m^2]
H_d daily diffuse irradiation, [W/m^2]
$\overline{H}_d$ monthly diffuse irradiation, [W/m^2]
H_{DM} average daily irradiation, [W/m^2]
H_0 extraterrestrial radiation on a horizontal surface in a daily basis, [W/m^2]
$\overline{H}_0$ extraterrestrial radiation on a horizontal surface in a monthly basis, [W/m^2]
h_1 head of the first tank
h_2 head of the second tank
I_T irradiation received by a tilted solar collector, [W/m^2]
I global irradiation, [W/m^2]
I_d diffuse irradiation, [W/m^2]
I_D diode current, [A]
I_{mp} PV generator current at maximum power point, [A]
$I_{mp,ref}$ PV generator current at maximum power point for reference temperature, [A]
I_{PH} photocurrent, [A]
I_{ref} reference radiation (1000 W/m^2), [W/m^2]
I_{S_1} first diode saturation current, [A]
I_{S_2} second diode saturation current, [A]
$I_{sc,ref}$ short circuit current at reference temperature, [A]
I_{sc} short circuit current, [A]
I_s diode saturation current, [A]

$I_{T,\mathrm{b}}$ beam radiation received by a tilted solar collector, [W/m^2]

$I_{T,r}$ reflected radiation received by a tilted solar collector, [W/m^2]

$I_{T,d\,iso}$ isotropic part of diffuse radiation received by a tilted solar collector, [W/m^2]

$I_{T,d\,cs}$ circumsolar part of diffuse radiation received by a tilted solar collector, [W/m^2]

$I_{T,d\,hz}$ horizon brightening part of diffuse radiation received by a tilted solar collector, [W/m^2]

I_x current corresponding to a voltage equal to one half of the open circuit voltage in the SANDIA ‘s PV module model, [A]

I_{xx} current corresponding to a voltage equal to the midway between the open circuit voltage and the maximum power point voltage in the SANDIA ‘s PV module model, [A]

I_0 extraterrestrial radiation on a horizontal surface in an hourly basis, [W/m^2]

I_{10} discharge current for a time of discharge equal to 10h, [A]

k boltzman coefficient [J/K]

k_T hourly clearness index, [-]

K_T daily clearness index, [-]

$\overline{K_T}$ monthly clearness index, [-]

$LPSPmax$ maximum loss of power supply probability, [-]

L_{st} location meridian, [°]

L_{loc} longitude of the location, [°]

m air mass, [-]

m_f ideality factor, [-]

n day of the year

N number of days in the month, [-]

N_{Batt} number of batteries, [-]

$N_{Batt,\max}$ maximum number of batteries, [-]

N_{DC} number of DC appliance, [-]

$N_{gen\max}$ maximum number of generations for Genetic Algorithm, [-]

N_{PV} number of PV module, [-]

$N_{PV,\max}$ maximum number of PV module, [-]

N_s number of batteries wire in series, [-]

p atmospheric pressure, [bar]

P_{AC} alternative current power, [kW]

P_{AC_0} alternative current reference power, [kW]

P_{DC} direct current power, [kW]

P_{DC_0} direct current reference power, [kW]

P_{PV} PV generator produced power, [W]

P_{PV_0} PV generator produced power at reference temperature, [W]
P_{mp} PV generator maximum power, [W]
$P_{mp,ref}$ PV generator maximum power, [W]
P_{so} required DC power to start the inversion process, [kW]
q elementary electron charge, [eV]
Q battery charge in the CIEMAT model, [Ah]
q_1 available charge, [Ah]
q_2 bound charge, [Ah]
$q_{1,0}$ initial amount of charge of the first tank, [Ah]
$q_{2,0}$ initial amount of charge of the second tank, [Ah]
$q_{\max}$ maximum amount of charge, [Ah]
$q_{T=t}$ amount of charge at time t, [Ah]
r_t ratio of hourly total radiation to daily total radiation, Collareis-Pereira ‘s model, [-]
R_b geometric factor, [-]
R_{ch} battery charging resistance, [Ω]
R_{disch} battery discharging resistance, [Ω]
R_S PV generator series resistance, [Ω]
R_{SH} PV generator shunt resistance, [Ω]
r_0 correction factor in the Hottel’s model, [-]
r_1 correction factor in the Hottel’s model, [-]
SOC_m maximum state of charge, [%]
t time, [s]
T temperature, [°C]
T_a ambient temperature, [°C]
T_c cell temperature, [°C]
T_{life} project lifetime, [y]
T_m module temperature, [°C]
T_{rep} converters, inverter and batteries lifetime, [y]
T_0 reference temperature, [°C]
V voltage, [V]
V_c charging voltage, [V]
V_d discharge voltage, [V]
V_{DC-bus} DC bud voltage, [V]
V_D diffuse voltage, [V]

V_{ec} final charge voltage, [V]
V_{g} gassing voltage, [V]
V_{mp} PV generator voltage at maximum power point, [V]
$V_{mp,ref}$ PV generator voltage at maximum power point for reference temperature, [V]
$V_{oc,ref}$ open circuit voltage at reference temperature, [V]
V_{oc} open circuit voltage, [V]
V_{T} threshold voltage, [V]
V_{o} operating voltage, [V]
WS Wind speed, [m/s]

Greek character

α_S solar altitude, [°]
β solar collector tilted angle, [°]
$\beta_{V_{oc}}$ open circuit voltage temperature coefficient in the PV module model of SANDIA laboratory, [-]
$\beta_{V_{mp}}$ maximum power voltage temperature coefficient in the PV module model of SANDIA laboratory, [-]
δ declination angle, [°]
ΔT is the temperature difference between the cell and the module back surface temperature at an irradiance of 1000 W/m^2 in the SANDIA 's PV module model, [°C]
ΔW_G amount of energy absorbed or emitted by the electron to cross the forbidden zone, [J]
γ azimuth angle, [°]
γ_S solar azimuth angle, [°]
η PV generator efficiency, [-]
μ PV generator temperature coefficient, [-]
η_0 PV generator efficiency at reference temperature, [-]
$\mu_{V_{OC}}$ PV generator voltage temperature coefficient, [-]
$\mu_{I_{SC}}$ PV generator current temperature coefficient, [-]
ω hourly solar angle, [°]
ω_s solar angle at sunset, [°]
ω_1 solar angle at the beginning of the hour, [°]
ω_2 solar angle at end of the hour, [°]
θ angle of incidence, [°]
θ_z azimuth angle, [°]

$\overline{\theta}$ hourly average angle of incidence, [°]
$\overline{\theta_z}$ hourly average azimuth angle, [°]
ϕ latitude, [°]
τ_b atmosphere transmittance of beam radiation, [-]
τ_d atmosphere transmittance of diffuse radiation, [-]
ρ_g albedo, [-]
η_c charging battery efficiency, [%]
τ time constant of the overcharge, [s]
η_{conv_bid} bidirectional converter efficiency, [%]

INTRODUCTION

0.1 General Status

More than one billion people in the world have no access to electricity and water. In 2009, the number of people without electricity was 1.4 billion which represents 20% of the world's population as shown in Figure 0.1.

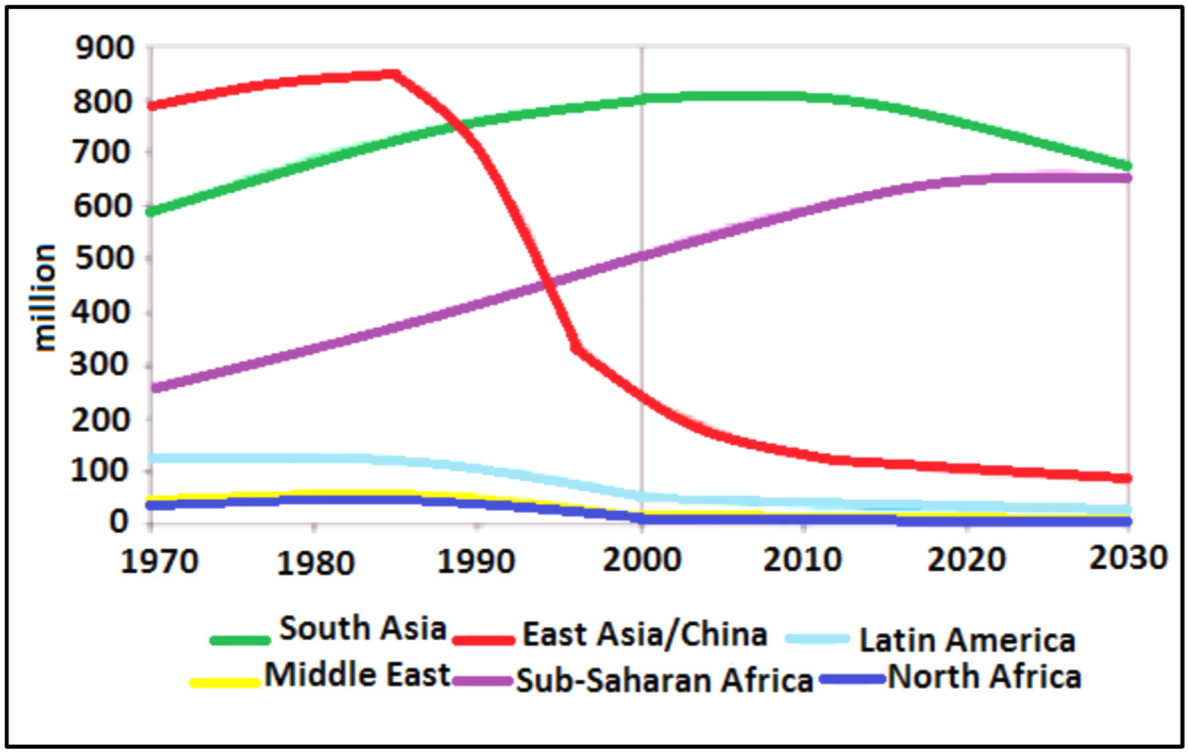

Figure 0.1: Number of people without electricity
1970-2030 -from (Girona, Szabo & Bhattacharyyam, 2016)

Nearly 85% of this population is in rural areas of Africa and South Asia. To solve this issue, most of the Sub-Saharan countries build their energy policies on a grid extension. Policies that cannot be supported by their electrical networks, that are in most of the time damaged and which require major renovations. Figure 0.2-A shows the percentage of transmission lines

which are more than 30 years old in several African countries. In most countries, the electrical network is more than 50 years old.

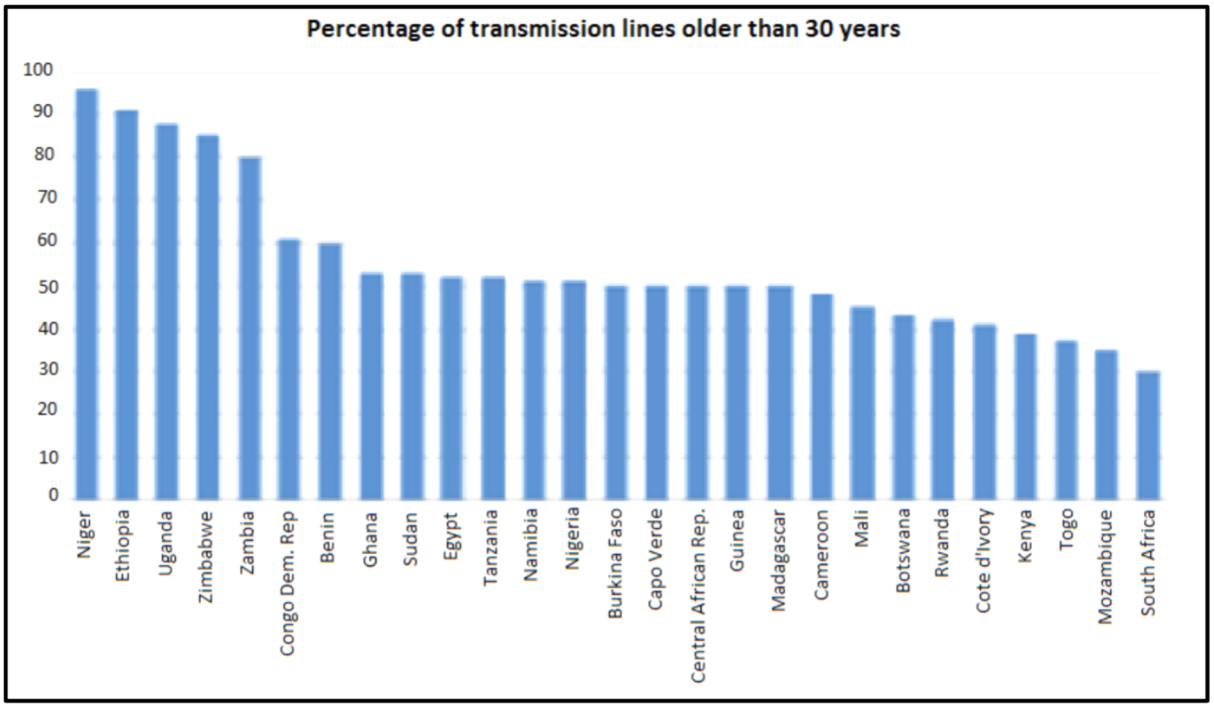

Figure 0.2 (A): Reliability of the electrical networks in Africa - from (Girona, Szabo & Bhattacharyyam, 2016)

Hence, it is not a surprise to find these countries in the list of the countries that are facing 10% or more black out time per year. Figure 0.2-B illustrates it.

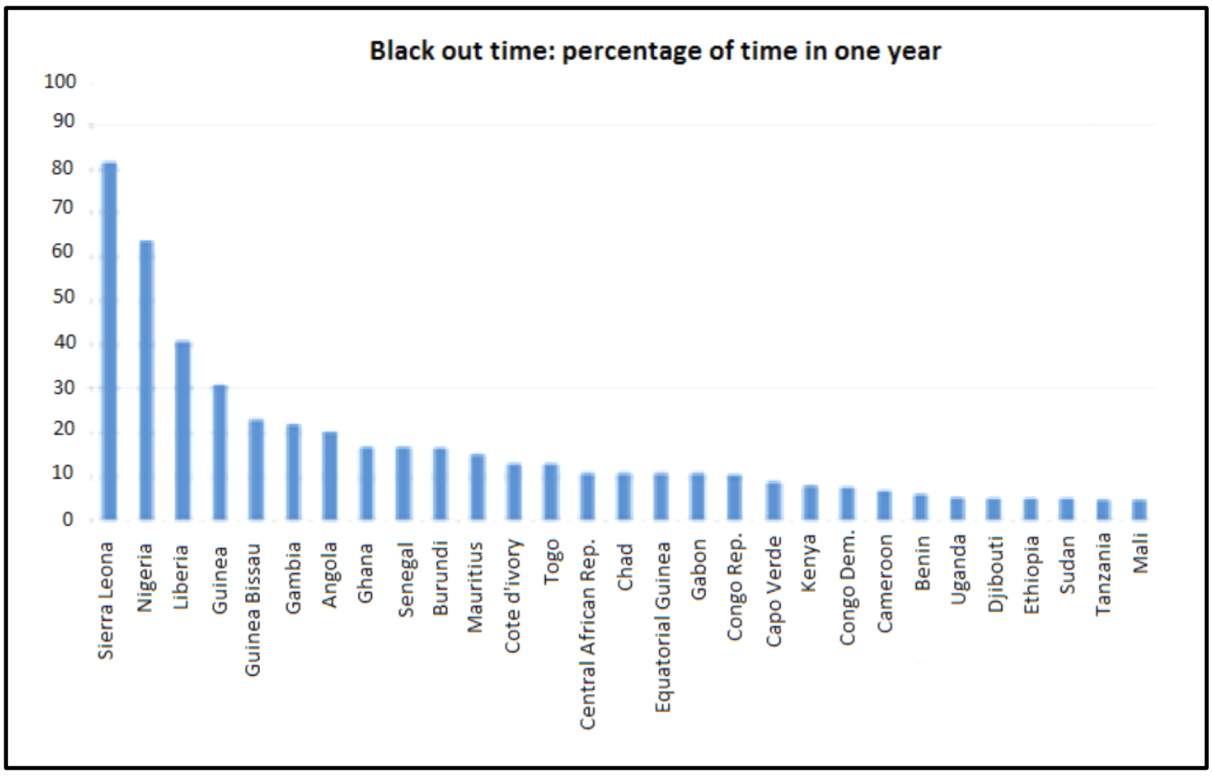

Figure 0.2 (B): Reliability of the electrical networks in Africa - from (Girona, Szabo & Bhattacharyyam, 2016)

Besides, the lack of maintenance, the dams draining during drought periods and the network destruction during conflicts are also partly, when not chiefly, at the origin of this situation. In addition, a grid extension would be more expensive than in developed countries. In fact, building new networks necessarily implies to build new roads to facilitate the access.

As a result, billions of dollars are spent by these countries without achieving the aimed result. The consequences are disastrous: increasingly harsh living conditions in rural areas encouraging a rural exodus which weakens rural areas and increases the demand of electricity in urban centers with the development of shantytowns in cities, failing of all the governmental actions in the fields of education, health and entrepreneurship and finally the increase of the insecurity. Thus, in 2018, electrification of remote areas is still a critical issue in lots of undeveloped countries.

0.2 Solar energy and its applications in Sub-Saharan Africa

Sub-Saharan Africa has a very good solar potential. Few regions in the world are as well doted in solar resource. In fact, several African countries have better solar potential than numbers of countries cited as leaders in the solar energy production. For example, Germany has an average solar irradiation of 1150 kWh/m^2/year while the solar irradiation of African countries oscillates between 1750 kWh/m^2/year and 2500 kWh/ m^2/year. Thirty-nine African countries have more 2000 kWh/m^2/year of irradiation. To take advantage of this solar potential, different applications exits.

The first application of solar system in Africa is the lighting. In fact, in several areas, habitants use candles and oil lamps to lighten their houses. The very low quality of light obtained by this means has an impact in different sectors: Education, Health and Economy. To solve this matter, more and more countries show interest in Solar Home Systems (SHSs). SHSs are made with PV panels coupled with batteries. Depending on the complexity of the
system, charge regulator, inverter or converter could be integrated. A better quality of life is achieved with these systems.
The second application is water pumping. It consists of PV modules couple with one or several pumps. The system generally integrates a tank to store the pumped water. The uselessness of batteries reduces the total cost of the system. The stored water is generally used for drinking, cooking and irrigating. These systems are very widely spread in North Africa.

The last application of PV systems is for industries and mines. In the mining sector, 15% to 20% of the total expands are for workforce and electricity. Diesel generators were generally used to satisfy this electricity demand. But nowadays, Diesel generators are coupled with PV panels. It reduces the use of the generator throughout the day which saves money for fuel expenses. South Africa is particularly advanced in these fields (Girona, Szabo & Bhattacharyyam, 2016).

With ever decreasing costs of systems (IRENA, 2017), using PV systems for electrification of remote areas represents a solution for the future. To support this revolution, researchers made available new models, designs control technics and new power management strategies, etc. These latter result in the development of programs and software tools that facilitate and optimize the design of PV systems. But a totally free access to the best of these tools and codes is not possible. In fact, for most of the available programs, a free access is provided for a limited period only. Thus, an unlimited free access program allowing the design of feasible, reliable and cost-effective PV systems for remote areas is still needed.

0.3 Project

The overall objective of this project is to develop a free access PV-battery system design program to facilitate energy provision in remote areas. The specific objectives are:

- to ensure accurate and precise modelling of the different components of the systems;
- to enable cost optimization;
- to make provision to distribute licences freely and allow access to the source-code;
- to implement the formulation in Python language;
- to allow modifications, enhancements, and updates of the data base.

0.4 Content

The first chapter of this thesis presents an overview of the relevant literature. In the second chapter an article entitled: “optimal design of PV-Battery system for decentralised electrification in Sub-Saharan Africa” is presented. This latter integrates the assumptions and different choices made to build the proposed program as well as a case of study performed in ELDORET. Discussions and recommendations are finally formulated in the fourth concluding chapter.

CHAPTER I

LITTERATURE REVIEW

1.1 PV solar generator

1.1.1. Solar cell technology

Most of the solar PV cells are made with silicon which is a semiconductor. Thus, the first part of this study focussed on a microscopic definition of the semiconductor. Secondly, a study of p-n junction made with silicon was done which lead to a proper definition of the solar cell. The contents of this preliminary study, inspired by the work of (Mertens, 2014) on solar PV systems is summarized in this section.

Considering an individual atom, Bohr postulates that the electron can only move in certain discrete shells also called level of energy. And the displacement of an electron from one shell to another occurs only with the absorption or the emission of an electromagnetic radiation. When several atoms are put together, their discrete shells combined to give energy band. And the transfer of electron now occurs between energy bands. Two types of band exist: conduction band and valence band. The valence band is where valence electrons are localised (electrons that are susceptible to link with other atoms 'electrons). The conduction band is the first unoccupied band. The space between them is called the forbidden zone (Figure 1.1).

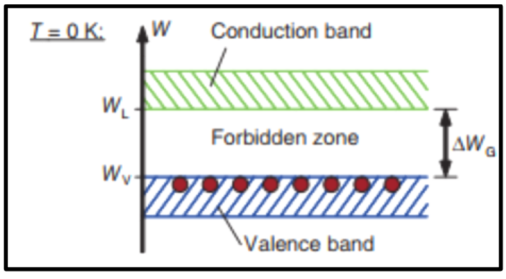

Figure 1.1 : Energy bands in crystal
- from (Konrad Mertens, 2014)

To cross the forbidden zone an amount of energy ΔW_G is absorbed or emitted. It is called bandgap. Depending on the width of the forbidden zone, three types of material are distinguished: insulators, conductors and semiconductors (Figure 1.2).

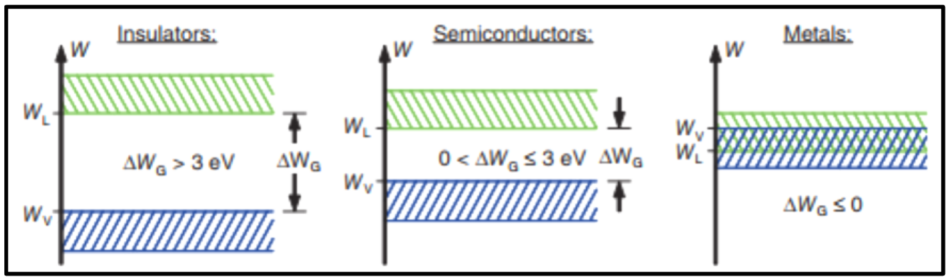

Figure 1.2: Description of energy band of insulators, conductors and semiconducters - from (Konrad Mertens, 2014)

Insulators are materials with a very big bandgap: typically, more than 3eV. Materials having a bandgap between 0 and 3eV are called semiconductors and materials with negative bandgap are conductors. Metals can be cited as perfect example of conductors.

Table 1.1: Different types of materials - from (Konrad Mertens, 2014)

Material	Type of material	Bandgap ΔW_G (eV)
Diamond	Insulator	1.3
Gallium Arsenide	Semiconductor	1.42
Silicon	Semiconductor	1.12
Germanium	Semiconductor	0.7

So, one can see that silicon is not the best conductor. To increase its conduction, a doping process is applied. This process consists of introducing foreign atoms into a semiconductor. One talks about n-doping when the foreign atom has more valence electrons than the origins atoms. If the foreign atom has less valence electron one talks about p-doping. In the silicon case, Phosphor is often used for n-doping and Boron for p-doping.

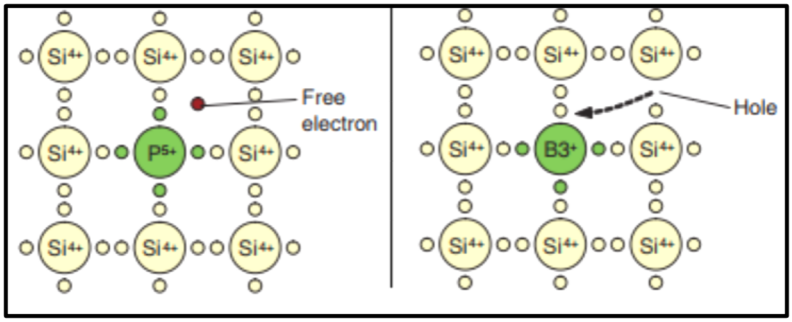

Figure 1.3: Phosphor and Boron respectively used
for n-doping and p-doping of the Silicon
- from (Konrad Mertens, 2014)

As showed in Figure 1.3, four Phosphor valence electrons link with four Silicon valence electrons. The remaining Phosphor electron is very weakly linked to the nucleus and thus considered as a free electron. It required a very few amounts of energy to transfer this electron to the conduction band. By repeating this process, the semiconductor gains a higher level of conductivity. Regarding the p-doping, the three Boron electron link with three Silicon electrons what leaves one unfilled hole. As a result, one obtains in one side a semiconductor electrically neutral with doped number of free electrons, and in the other side a semiconductor electrically neutral with doped number of holes. The combination of these latter gives a p-n junction.

Once the p-n junction is built, two phenomena take place. Due to the concentration gradient, the free electrons of the n-doped crystal migrate to the p-doped side to fill the hole. It creates a current called diffuse current. The doped crystals are then no longer electrically neutral. The n-doped side is now positively charged while the p-doped side is negatively charged. Due to the rising number of these charges, an electrical field comes into existence. The tendency of this field is to turn back the electrons and the holes to their initial position. This latter electron's displacement caused field current. Finally, the diffuse and the field current cancelled each other causing the creation of a space charged region at the p-n junction. Figure 1.4 perfectly illustrates this phenomenon.

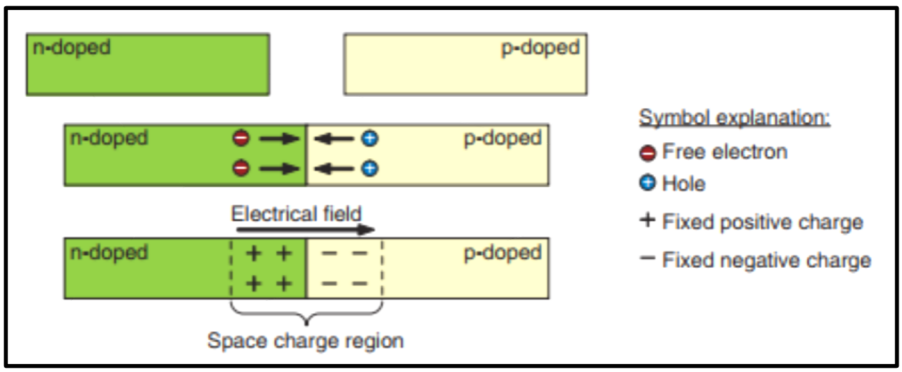

Figure 1.4: p-n junction - from (Konrad Mertens, 2014)

The difference of potential between the n-doped and the p-doped of the space charged region is called diffuse voltage V_D . When the p-n junction is illuminated, absorbed photons extract electron-hole pairs. Depending on the position of the generated pair, three scenarios can be considered. In the space charge region, the electron is separated from hole by the prevailing field. The electron is transferred in the n-doped region and the hole in the p-doped region. Being the majority carriers in these two respective regions, the probability of recombination is very low. Thus, they can easily flow to the contacts. The second scenario is an electron-hole pair located in the space extending 100um after the space charge region. In this case, the charge carrier firstly diffuses to the space charge region. If the pair was in the p-doped side, the electron will diffused. If it was in the n-doped side, the hole will diffused. The diffusion being relatively small, the charge carrier has great chance to reach the space charge region. Once this latter is reached, the first scenario is repeated. If the electron-hole pair extraction takes place beyond 100 um region, the charge carrier will unfortunately recombine before it can reached the space charge region. This migration process is illustrated in Figure 1.5

If a generator reference-arrow system is adopted to describe the previous phenomenon, a p-n junction is called PV solar cell. Otherwise, in load reference-arrow system it is called a photodiode. As showed in Figure 1.6.

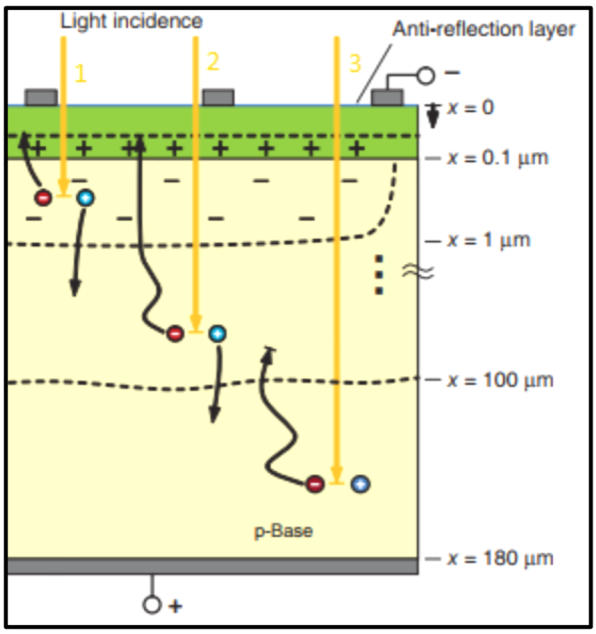

Figure 1.5: Electron migration description
- from (Konrad Mertens, 2014)

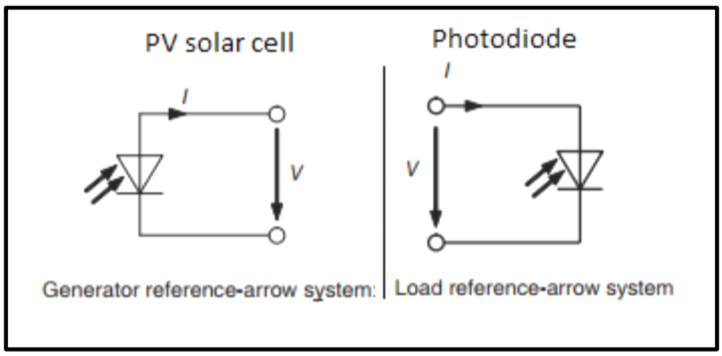

Figure 1.6: Solar cell and Photodiode
symbolic representations - from (Konrad Mertens, 2014)

1.1.2 PV generator modelling

1.1.2.1 Simple models

The following models are called simple because only manufacturer data are used for very basic mean of calculation. Several ones can be found in the literature; only three of them are presented in this work.

In the first model, the efficiency η is assumed to be a linear function which only depends on the cell temperature T_c. If η_0 is considered as the nominal efficiency given by the manufacturer and T_0 (25°C) the reference temperature at which this efficiency was measured, the PV generated power P_{PV} is then given by equation 1.1.

$$P_{PV} = \eta I_T = \eta_0[1-\mu(T_c - T_0)]I_T \tag{1.1}$$

In the case where the PV nominal power P_{PV_0} is given, a very closed model shown in equation 1.2 is used.

$$P_{PV} = \frac{I_T}{1000}\eta P_{PV_0} = \frac{I_T}{1000}[1-\mu(T_c - T_0)]P_{PV_0} \tag{1.2}$$

The third model was proposed by (Lasnier and Gan 1990). It consists of a linear model for the calculation of the maximum power P_{mp}. The voltage and the current temperature coefficients $\mu_{V_{OC}}$ and $\mu_{I_{SC}}$ are required to calculate the voltage and the current at the maximum power point. These latter are given by the equations 1.3,1.4 and 1.5.

$$P_{mp} = V_{mp} I_{mp} \tag{1.3}$$

$$V_{mp} = V_{mp,ref} + \mu_{V_{OC}}(T_c - T_{c,ref}) \tag{1.4}$$

$$I_{mp} = I_{mp,ref} + I_{sc,ref}(\frac{\overline{I_T}}{I_{ref}}) + \mu_{I_{SC}}(T_C - T_{C,ref}) \quad (1.5)$$

1.1.2.2 Electrical model

To predict the power generated by a PV module under certain condition, three electrical equivalent circuits were developed (Mertens, 2014): a simplified model, a standard model also called five parameter model and a two diodes model. The simplified electrical model (Figure 1.7) assumes that a PV solar cell can be modelled as a current generator wires in parallel with a diode.

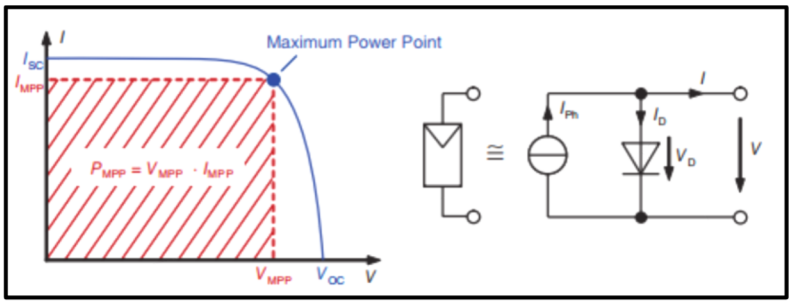

Figure 1.7: Solar cell simplified electrical model
-from (Konrad Mertens, 2014)

The main equation expressing this model is the equation 1.6:

$$I = I_{PH} - I_D = I_{PH} - I_S * (e^{(\frac{V}{m_f V_T})} - 1) \quad (1.6)$$

where I_{PH}, the photocurrent, I_s the diode saturation current, m_f an ideality factor allowing to be closer to reality and V_T the voltage temperature defined by the equation 1.7.

$$V_T = \frac{k * \mathrm{T}}{q} \quad (1.7)$$

To go deeper into electrical losses, the standard model also called a five parameters model (Figure 1.8) – was built. In this latter, series resistances R_S are used to model ohmic losses. Leak current at the edge of the solar cell are modelled with the shunt resistance R_{SH}. The current is given by the equation 1.8.

$$I = I_{PH} - I_D - I_{SH} \tag{1.8}$$

where I_{SH} is found as: $I_{SH} = \frac{V + IR_S}{R_{SH}}$ (Mertens, 2014)

So, the current I becomes in equation 1.9.

$$I = I_{PH} - I_S * (e^{(\frac{V+IR_S}{mV_T})} - 1) - \frac{V + IR_S}{R_{SH}} \tag{1.9}$$

Due to its implicit form this equation can only be solved numerically. A complete resolution process is presented by (Duffie and Beckman, 2014).

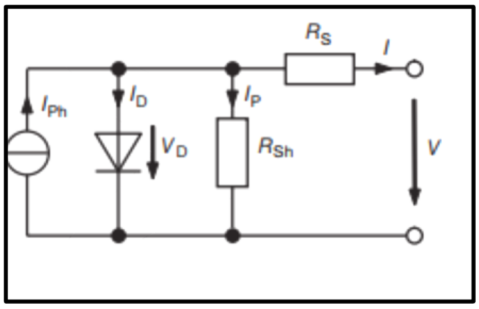

Figure 1.8: Standard model
or five parameters model
-from (Konrad Mertens, 2014)

The electron-hole pair recombination process is supposed to be inexistent in the standard model. It was considered in the two diodes model (Figure 1.9). The first diode with an ideality

factor of 1 represents the diffuse current. The second one with the ideality factor of 2 represents the recombination current.

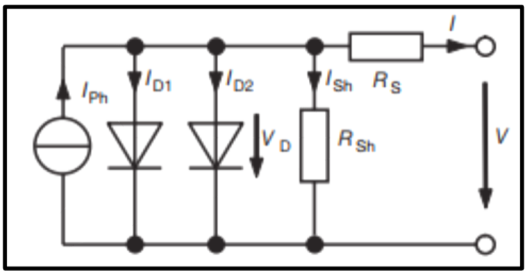

Figure 1.9: Two diodes model
-from (Konrad Mertens, 2014)

The characteristic curve equation becomes the equation 1.10.

$$I = I_{PH} - I_{S_1} * (e^{\frac{V+IR_S}{V_T}} - 1) - I_{S_2} * (e^{\frac{V+IR_S}{2.V_T}} - 1) - \frac{V + I.R_S}{R_{SH}} \qquad (1.10)$$

The complexity of its solving process made the two diodes model unsuitable to use in PV system yearly simulation. It is mostly used in the research laboratory where more level precision is needed.

1.1.2.3 Sandia PV array Performance model

Sandia proposes an empirical array performance model. In their 2004 report (King, Boyson & Kratochvill, 2004), they presented the modelling and the testing of a 165-Wp multi-crystalline silicon module. It took place in Albuquerque during the month of January with both clear and cloudy operating conditions. The model is based on the determination of five different points of the I-V characteristic curve of the studied module as shown in Figure 1.10.

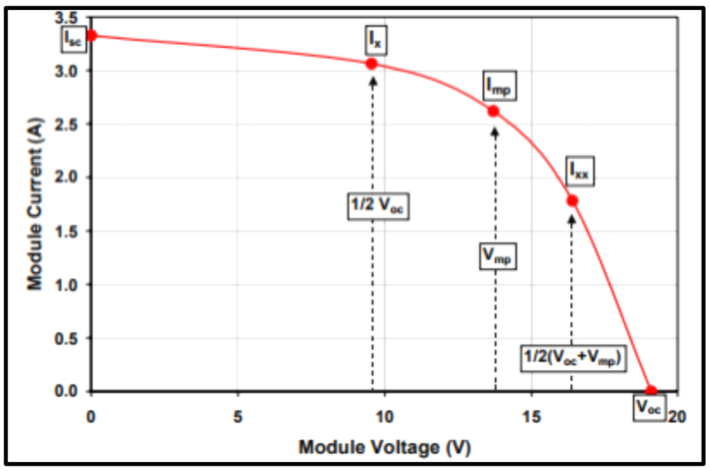

Figure 1.10: Module I-V curve showing the
5 points given by the Sandia performance model
-from (King, Boyson & Kratochvill, 2004),

The first three points correspond to the short circuit current I_{sc}, the open circuit voltage V_{oc} and the maximum point I_{mp}, V_{mp}. The fourth and fifth equations are defined by their currents I_x and I_{xx} and their voltages which respectively correspond to one half of the open circuit voltage $(\frac{1}{2}V_{oc})$ and the midway between the open circuit voltage and the maximum power point voltage $(\frac{1}{2}(V_{oc}+V_{mp}))$ The Fill Factor FF and the maximum power P_{mp} are then deduced. In these equations, four different aspects are considered: the solar irradiance, the solar resources, the standard conditions and temperature.

A couple of coefficients are defined to account for the solar irradiance influence. They are empirically determined to relate the effective solar irradiance E_e respectively to I_{mp}, V_{mp}, I_x and I_{xx}.

Concerning the solar resources, two empirical functions are used. The function $f_1(AM_a)$ quantifies the influence of the solar spectral on I_{sc}. The second function $f_2(\text{AOI})$ quantifies

the optical influence on I_{sc}. Series of tests are performed to determine their polynomial forms which are (King, Boyson & Kratochvill, 2004) given by the equations 1.11 and 1.12.

$$f_1(AM_a) = a_0 + a_1 * AM_a + a_2 * (AM_a)^2 + a_3 * (AM_a)^3 + a_4 * (AM_a)^4 \quad (1.11)$$

$$f_2(AOI) = b_0 + b_1 * AOI + b_2 * (AOI)^2 + b_3 * (AOI)^3 + b_4 * (AOI)^4 + b_5 * (AOI)^5 \quad (1.12)$$

The standard conditions are taken for a solar irradiance of 1000 W/m^2, a temperature of 25°C, an air mass of 1.5 and an angle of incidence of 0°.

Regarding the temperature, SANDIA (King, Boyson & Kratochvill, 2004) proposes to first calculate the back-surface module temperature T_m with the equation 1.13:

$$T_m = E_i * [e^{a+b*WS}] + T_a \quad (1.13)$$

where T_a is the ambient temperature, WS the wind speed measured at 10 m of height, E_i the measured irradiance and a and b empirically determined coefficients.
The cell temperature is obtained with the equation 1.14:

$$T_c = T_m + \frac{E}{E_o} * \Delta T \quad (1.14)$$

where ΔT is the temperature difference between the cell and the module back surface temperature at an irradiance of 1000 W/m^2. The empirically determined coefficients were determined for certain module types and mounting configurations in T_a (Table 1.2).

Table 1.2: Empirically determined coefficient were determined for certain module types and mounting configuration -from (King, Boyson & Kratochvill, 2004)

Module Type	Mount	a	b	ΔT (°C)
Glass/cell/glass	Open rack	-3.47	-0.0594	3
Glass/cell/glass	Close roof mount	-2.98	-0.0471	1
Glass/cell/polymer sheet	Open rack	-3.56	-0.0750	3
Glass/cell/polymer sheet	Insulated back	-2.81	-0.0455	0
Polymer/thin-film/steel	Open rack	-3.58	-0.113	3
22X Linear Concentrator	Tracker	-3.23	-0.13	13

Once the temperature is calculated, its influence on the cell's behaviour is implemented by use of temperature coefficients. SANDIA (King, Boyson & Kratochvill, 2004), proposes four temperature coefficients: $\alpha_{I_{sc}}$, $\alpha_{I_{mp}}$, $\beta_{V_{oc}}$ and $\beta_{V_{mp}}$. They respectively represent the normalized temperature coefficient for I_{sc}, the normalized temperature coefficient for I_{mp}, the temperature coefficient for the module open circuit voltage V_{oc} as a function of the effective irradiance and the temperature coefficient for module maximum power voltage V_{mp} as a function of the effective irradiance. SANDIA supposes that taking the same temperature coefficient for I_{mp} and I_{sc} or for V_{mp} and V_{oc} ,as in the five parameter model, is erroneous. If not procured by the manufacturer, the four different coefficients must be measured. The whole model equations are presented in APPENDIX A.

1.2 POA (Plane of Array): Radiation modelling

1.2.1 Definitions

Several definitions used in the literature to study the different aspect of solar radiation are needed to understand the gist of the code that was implemented herein. The material presented here was taken from the work of (Duffie and Beckman, 2014).

The solar constant G_{SC} is the annual average of incident radiation received from the sun outside the earth atmosphere per surface unit. It is estimated at about 1367 W/m^2. The daily extraterrestrial radiation incident on a plane surface is noted G_{on}. Its value is given the equation 1.15.

$$G_{on} = G_{SC} * (1 + 0.0033 * \cos\frac{360n}{365}) \tag{1.15}$$

where *n* is the day of the year

For calculation linked to the position of the sun the standard time is not enough representative. Thus, the solar time is used. It is deduced from the standard time by applying two corrections. The first one is linked to the difference in longitude between the local standard time-based meridian and the observer's meridian. The second one is from equation time. It gives the equation 1.16.

$$\text{Solar Time} = \text{Standard Time} + 4(L_{st} - L_{loc}) + E_t \tag{1.16}$$

where L_{st} is the local meridian for the local time and L_{loc} is the longitude of the location. E_t is the equation of time which is given by the equation 1.17.

$$\begin{aligned} E_t = {} & 229.2 * (0.000075 + 0.001868 * \cos B - 0.032077 * \sin B \\ & -0.014615 * \cos 2B - 0.04089 * \sin 2B) \end{aligned} \tag{1.17}$$

where *B* defined the equation 1.18.

$$B = (n-1)\frac{360}{365} \tag{1.18}$$

From the solar time is deduced the hourly solar angle ω with the equation 1.19.

$$\omega = 15 * (\text{Solar Time}) \tag{1.19}$$

The Air mass m is the ratio of the mass of air traverse by the beam radiation at any moment and any location. It is calculated with the equation 1.20.

$$m = \frac{1}{\cos\theta_z} \tag{1.20}$$

where θ_z is the azimuth angle defined later.

To describe the geometric relationship between the sun position and the earth, several angles must be used (Figure 1.11). The declination angle δ is the angular position of the sun to the solar noon. It is calculated with the equation 1.21.

$$\delta = 23.45 * \sin(360\frac{284+n}{365}) \tag{1.21}$$

The latitude ϕ is the angular position in the north and the south of the equator. $-90^o \le \phi \le 90^o$. The slope β is the angle formed by the PV array with the horizontal. $0^o \le \beta \le 180^o$. The azimuth angle γ is the horizontal projection of the angle between normal to the surface and the south. γ_S is the solar azimuth angle. It is given by the equation 1.22.

$$\gamma_s = sign(\omega)\left|\cos^{-1}(\frac{\cos\theta_z \sin\phi - \sin\delta}{\sin\theta_z \cos\phi})\right| \tag{1.22}$$

The angle of incidence θ is the angle between beam radiation and the normal to the surface. It is given by the equation 1.23.

$$\cos\theta = \sin\delta\sin\phi\cos\beta - \sin\delta\sin\phi\sin\beta\cos\gamma + \cos\delta\cos\phi\cos\beta\cos\omega + \cos\delta\sin\phi\sin\beta\cos\gamma\cos\omega + \cos\delta\sin\beta\sin\gamma\sin\omega \quad (1.23)$$

The zenith angle θ_z is the angle between the line to the sun and the vertical. Its complementary α_S is the angle between the line to the sun and the horizontal. The angle of incidence is equal to the zenith angle for horizontal surface. This comes to put β equal to zero in the previous equation. It gives the equation 1.24.

$$\cos\theta_z = \cos\phi\cos\delta\cos\omega + \sin\phi\sin\delta \quad (1.24)$$

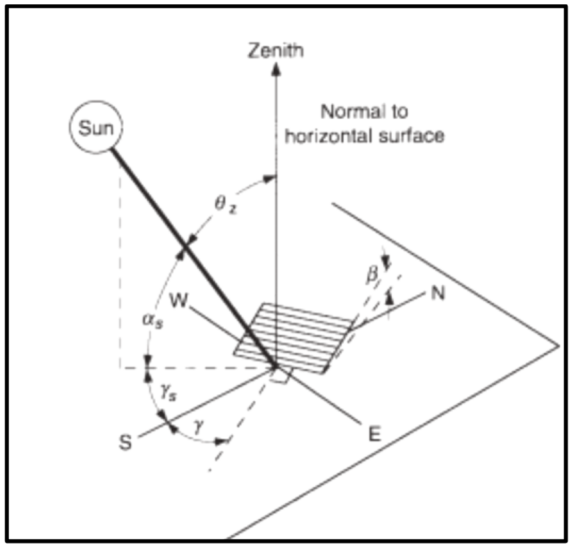

Figure 1.11: Solar angle
-from (Duffie & Beckman, 2014)

1.2.2 Estimation of solar Radiation

The extraterrestrial radiation calculated upper is not totally transferred to the earth. In fact, one part of this energy is absorbed by the atmosphere, deviated or scattered. This is called the diffuse radiation. The other part which directly reached the earth surface is the beam radiation.

Different empirical models were developed to estimate these two entities in an hourly, daily or monthly basis.

1.2.2.1 Beam and Diffuse radiation estimation

(Hottel, 1976) presents a model to calculate the beam radiation through the atmosphere. It is based on the calculation of the atmosphere transmittance for beam radiation τ_b which is the ratio of beam radiation to the extraterrestrial radiation on a horizontal surface. It is given by the equation 1.25.

$$\tau_b = a_o + a_1 * e^{\frac{-k}{\cos\theta_z}} \tag{1.25}$$

The constants a_0, a_1 and k are calculated for a standard atmosphere with 23 km of visibility. They are deduced from the reference constants a_0^*, a_1^* and k^* that are drawn from the equations 1.26, 1.27 and 1.28.

$$a_0^* = 0.4237 - 0.00821 * (6 - A)^2 \tag{1.26}$$

$$a_1^* = 0.5055 - 0.00595 * (6.5 - A)^2 \tag{1.27}$$

$$k^* = 0.2711 - 0.01858 * (2.5 - A)^2 \tag{1.28}$$

where A is the altitude in km

In the Table 1.3 are given the correction factors $r_0 = \frac{a_0}{a_0^*}$, $r_1 = \frac{a_1}{a_1^*}$ and $r_k = \frac{k}{k^*}$.

Table 1.3: Correction factor -from (Duffie & Beckman, 2014)

Climate Type	r_0	r_1	r_k
Tropical	0.95	0.98	1.02
Midlatitude summer	0.97	0.99	1.02

Subarctic summer	0.99	0.99	1.01
Midlatitude winter	1.03	1.01	1.00

Keeping the same line, (Kreith and Kreider, 1978) proposed a different atmosphere transmittance for beam radiation τ_b. In this case, the curvature of the light rays is considered. It is obtained with the equations 1.29, 1.30 and 1.31.

$$\tau_b = 0.5 * (e^{-0.65\,\mathrm{m(z,\theta_z)}} + e^{-0.095 m(z,\theta_z)}) \tag{1.29}$$

$$m(z,\theta_z) = m(0,\theta_z)\frac{p(\mathrm{z})}{p(0)},\ p: atmospheric\ \ pressure \tag{1.30}$$

$$m(0,\theta_z) = \sqrt{1229 + (614\cos\theta_z)^2} - 614\cos\theta_z \tag{1.31}$$

After estimating the beam radiation, it is important to calculate the diffuse radiation on a horizontal surface and then deduce the total radiation. (Liu and Jordan, 1960) bring out an empirical relation between the atmosphere transmittance for beam and diffuse radiation τ_b and τ_d. Equation 1.32 traduce this model.

$$\tau_d = \frac{I_d}{I_0} = 0.271 - 0.294 * \tau_b \tag{1.32}$$

Thus, by combining Liu and Jordan model and Hottel model, one can deduced the total irradiation on a plane surface.

1.2.2.2 Correlation of Erbs

With the advance measurement's techniques, other researchers tried to establish more precise models. It is the case of (Erbs and al, 1980). To estimate the ratio of hourly diffuse radiation, they proposed to correlate the hourly clearness k_T and the diffuse fraction $\frac{I_d}{I}$. I_d and I being

respectively: the diffuse radiation on a plane surface and the hourly total radiation. k_T is defined by equation 1.33.

$$k_T = \frac{I}{I_0} \tag{1.33}$$

where I_0 the extraterrestrial radiation on a horizontal surface for an hour period. It is calculated with the equation 1.34.

$$I_0 = \frac{12*3600}{\pi} G_{sc}(1+0.033\cos\frac{360n}{365})[\cos\phi\cos\delta(\sin\omega_2 - \sin\omega_1) + \frac{\pi(\omega_2-\omega_1)}{180}\sin\phi\sin\delta] \tag{1.34}$$

The Erbs and al correlations are shown in the equation 1.35.

$$\frac{I_d}{I} = \begin{cases} 1-0.09k_T & for\ k_T \le 0.22 \\ 0.9511-0.1604+4.388k_T^2-16.638k_T^3+12.336k_T^4 & for\ 0.22 < k_T \le 0.8 \\ 0.165 & for\ k_T > 0.8 \end{cases} \tag{1.35}$$

The same correlation is also available in a daily or monthly basis with K_T the daily clearness and $\overline{K_T}$ the monthly clearness. They are respectively defined as the ratio of the total radiation H to the extraterrestrial radiation on a horizontal surface H_0 in a daily basis and the ratio of the monthly global radiation $\overline{H}$ to the extraterrestrial radiation on a horizontal surface $\overline{H_0}$ in a monthly basis. H_0 and $\overline{H}_0$ given by the equation 1.37.

$$H_0 = \frac{24*3600*G_{SC}}{\pi}(1+0.033\cos\frac{360n}{365})[\cos\phi\cos\delta\sin\omega_s + \frac{\pi\omega_s}{180}\sin\phi\sin\delta] \tag{1.36}$$

$$\overline{H_0} = \frac{\sum_{i=1}^{N} H_{0,i}}{N} \tag{1.37}$$

where N is the number of days in the month and $H_{0,i}$ the extraterrestrial irradiation at the ith day of the month. Knowing the value of K_T, if the sunset hour angle ω_s is inferior or equal to 81.4, the correlation is given the equation 1.38.

$$\frac{H_d}{H} = \begin{cases} 1 - 0.2727K_T + 2.4495{K_T}^2 - 11.9514{K_T}^3 + 9.3879{K_T}^4 & for\ K_T < 0.715 \\ 0.143 & for\ K_T \geq 0.715 \end{cases} \tag{1.38}$$

Otherwise the equation 1.38.

$$\frac{H_d}{H} = \begin{cases} 1 + 0.2832K_T - 2.5557{K_T}^2 + 0.8448{K_T}^3 & for\ K_T < 0.715 \\ 0.175 & for\ K_T \geq 0.715 \end{cases} \tag{1.39}$$

In a monthly basis, the calculation of $\overline{K_T}$ leads to the equation 1.40.

$$\frac{\overline{H_d}}{\overline{H}} = \begin{cases} 1.391 - 3.560\overline{K_T} + 4.189{\overline{K_T}}^2 - 2.137{\overline{K_T}}^3 & for\ \omega_s \leq 81.3\ and\ 0.3 \leq \overline{K_T} \leq 0.8 \\ 1.311 - 3.022\overline{K_T} + 3.427{\overline{K_T}}^2 - 1.821{\overline{K_T}}^3 & for\ \omega_s > 81.3\ and\ 0.3 \leq \overline{K_T} \leq 0.8 \end{cases} \tag{1.40}$$

Thus, Erbs and al. correlation allows calculating the diffuse radiation by knowing the clearness. The beam radiation is then deduced by subtracting the diffuse part from the global radiation. Most of the time, hourly correlation is used as this latter insured to have more precise results. But, most of the time, due to the lack of data, only daily or even monthly global radiations are available. To solve this issue, (Collares-Pereira & Rabl, 1979) propose a method to deduce the hourly total radiation I from the daily total radiation H. The ration of hourly total radiation to daily total radiation r_t is firstly calculated by the equations 1.41, 1.42 and 1.43.

$$r_t = \frac{\pi}{24}(a + b\cos\omega)\frac{\cos\omega - \cos\omega_s}{\sin\omega_s - \frac{\pi\omega_s}{180}\cos\omega_s} \quad (1.41)$$

$$a = 0.409 + 0.5016 * \sin(\omega_s - 60) \quad (1.42)$$

$$b = 0.6609 - 0.4767 * \sin(\omega_s - 60) \quad (1.43)$$

Then knowing H , I is deduced.

1.2.2.3 Radiation on sloped surface

Till now, all the calculations were done for horizontal surface. But, especially for PV installations, the surface in question is sloped. So, it is very important to know the solar radiation incident on a tilted surface. In this case, not only the diffuse and beam radiation are considered. The radiation reflected from different surfaces "seen" by the tilted surface is included. As showed in Figure 1.12, the diffuse radiation is separated in three parts: the isotropic part $I_{T,d\,iso}$ received uniformly, the circumsolar diffuse part $I_{T,d\,cs}$ and the part coming from horizon brightening $I_{T,d\,hz}$.

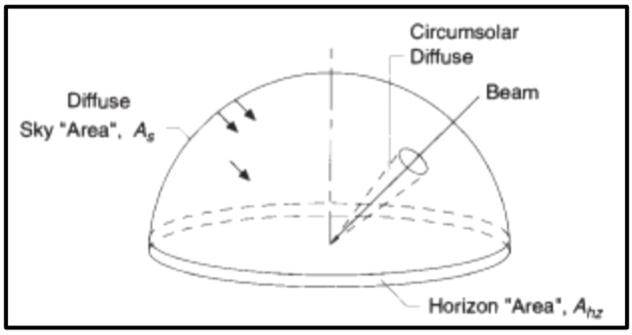

Figure 1.12: Diffuse radiation model
for tilted surface -from (Duffie & Beckman, 2014)

So, the radiation on a tilted surface I_T is given by the equation 1.44.

$$I_T = I_{T,\mathrm{b}} + I_{T,d\,iso} + I_{T,d\,cs} + I_{T,d\,hz} + I_{T,r} \tag{1.44}$$

where $I_{T,\mathrm{b}}$ and $I_{T,\mathrm{r}}$ respectively: the beam radiation on tilted surface and the reflected radiation on the tilted surface.

This equation can also be written like equation 1.45.

$$I_T = I_b R_b + I_{d,iso} F_{c-s} + I_{d,cs} R_b + I_{d,hz} F_{c-hz} + I \rho_g F_{c-g} \tag{1.45}$$

where F_{c-s}, F_{c-hz} and F_{c-g} respectively the view factor from the sky to the collector, the view factor from the horizon to the collector and the view factor from the ground to the collector. ρ_g is the albedo. The geometric factor R_b, the ratio of beam radiation on tilted surface to that of a horizontal surface at any time, can be calculated with the equation 1.46.

$$R_b = \frac{I_{T,b}}{I_{hor,b}} \approx \frac{\cos\overline{\theta}}{\cos\overline{\theta_z}} \tag{1.46}$$

The different models found in the literature aimed to explicitly define the view factors. The simplest model is the isotropic sky model (Shukla, Rangnekar & Sudhakar, 2015). In this latter, only the isotropic share of the diffusion radiation is considered. It is given by the equation 1.47.

$$I_T = I_b R_b + I_d * (\frac{1+\cos\beta}{2}) + I * \rho_g (\frac{1-\cos\beta}{2}) \tag{1.47}$$

where β is the tilted angle.

An anisotropic model proposed by (Hay and Davies, 1980) separates the diffuse in two parts: the isotropic and the circumsolar. The diffuse radiation is written is obtained from with equation 1.48:

$$I_{d,T} = I_{T,d\,iso} + I_{T,d\,cs} = I_d[(1-A_i)(\frac{1+\cos\beta}{2}) + A_i R_b] \quad (1.48)$$

where A_i is the anisotropic index which is given by the equation 1.49.

$$A_i = \frac{I_b}{I_0} \quad (1.49)$$

The total radiation on a tilted surface is then given by the equation 1.50.

$$I_T = (I_b + I_d A_i)R_b + I_d(1-A_i)(\frac{1+\cos\beta}{2}) + I\rho_g(\frac{1-\cos\beta}{2}) \quad (1.50)$$

To take into account the horizon brightening, (Reindl and al., 1988) add a modulating factor $1 + f\sin^3(\frac{\beta}{2})$ where f is defined by the equation 1.51.

$$f = \sqrt{\frac{I_b}{I}} \quad (1.51)$$

The diffuse on a tilted surface is given by the equation 1.52.

$$I_{d,T} = I_d[(1-A_i)(\frac{1+\cos\beta}{2})(1+f\sin^3(\frac{\beta}{2})) + A_i R_b] \quad (1.52)$$

So, the complete model named as HDKR (Hay, Davies, Klutcher and Reindl) gives the equation 1.53.

$$I_T = (I_b + I_d A_i) R_b + I_d (1 - A_i)(\frac{1+\cos\beta}{2})(1 + f \sin^3(\frac{\beta}{2})) + I\rho_g(\frac{1-\cos\beta}{2}) \qquad (1.53)$$

Battery

1.3 Battery technology

A deep description of the different phenomena and reactions occurring into batteries was made by (Mark, 2014). A summary of this work is provided is in this paragraph. Batteries are made with electrochemical cells. They convert chemical energy into electricity. Battery cells are made with two electrodes deepen in an electrolyte solution. The current flows when the circuit is closed. Chemical reactions occurring between the electrodes and the electrolyte made current flows. The electrodes and the electrolyte might differ depending on the types of batteries. In the market can be found: lead acid batteries, lithium ion, nickel metal hybrid and nickel cadmium. Lead acid battery being more readily available and cost effective, its use is more suitable for remote area. For this latter, the redox reaction operates between lead dioxide plate (PbO_2), a negative lead plate (Pb) and an electrolyte composed with of sulphuric acid (H_2SO_4).

$$Pb + PbO_2 + 2H_2SO_4 \underset{\text{Discharge} \rightarrow}{\overset{\leftarrow \text{Charge}}{\Leftrightarrow}} 2PbSO_4 + 2H_2O \qquad (1.54)$$

During the charging, lead dioxide is produced on the positive plate, lead is produced on the negative plate and the amount of sulphuric acid increased. When the battery is being discharged, lead sulphate is produced, and the water increased. When fully charged, the cell battery voltage is 2.1 V.

A battery can store a certain amount of energy which is its capacity. Transmitted by the manufacturer, it is measured in Ah. Its value varies with the rate at which the battery is discharge. A discharge current of 1amp might deliver 100 Ah which give a capacity of 100Ah.

The same battery which discharges with a current of 4 amps has a rated capacity of 80Ah. But the whole capacity of the battery can't be used. A depth cycle battery should not be discharged below 60%. The admissible minimum level of energy is called maximum depth of discharge (DoD_{max}). To insured that this threshold is not reached, the state of charge (SOC) of the battery must be controlled. Beyond its discharge, the battery loses charge by a process called self-discharge.

An overcharge occurs when a battery at 100% of state of charge is still in charge. Continued overcharge can reduce the lifetime of the battery. In fact, the excess current causes a reaction into the battery that converts the water in hydrogen. This decreases the amount of electrolyte and liberates explosive hydrogen gas in the air. To avoid this phenomenon, a charge controller is always connected between the battery and PV array or the DC bus depending on the configuration of the system.

1.3.1 Battery modelling

In general, a battery is viewed as a voltage source in series with a resistance, as illustrated in Figure 1.13. Depending on the required level of precision, different approach can be found. Analytical model have the advantage to be general, but some taken hypothesis makes the obtained solutions non-representative of the whole reality. In parallel, empirical models based on experimental results exist. Most of them required parameters that are not given by the manufacturer. Three different models are exposed in this review: the KiBaM model (Manwell & McGowan, 1993), the CIEMAT model (Coppeti, Lorenzo & Chenlo, 1993) and the Pspice model (Ameen, Pasupuleti & Khatib, 2015).

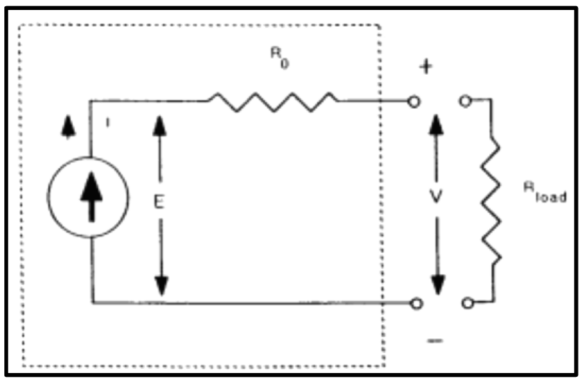

Figure 1.13: Battery electrical schematic
-from (Coppeti, Lorenzo & Chenlo, 1993)

1.3.1.1 Kinetic Battery Model (KiBaM)

The KiBaM model (Manwell & McGowan, 1993) is based on the chemical kinetics' behaviour of the battery. The voltage source is modelled as two tanks separated with a conductance. The immediately available charge is modeled as a tank having a capacity, q_1. The bound charge is represented by a second tank with a capacity q_2. The equations 1.55 and 1.56 traduce this modelling.

$$\frac{dq_1}{dt} = -I_{bat} - k'(h_1 - h_2) \tag{1.55}$$

$$\frac{dq_2}{dt} = k'(h_1 - h_2) \tag{1.56}$$

where I_{bat} is the constant current during a time step, k' the conductance, h_1 and h_2 the heads of the two tanks (Figure 1.14).

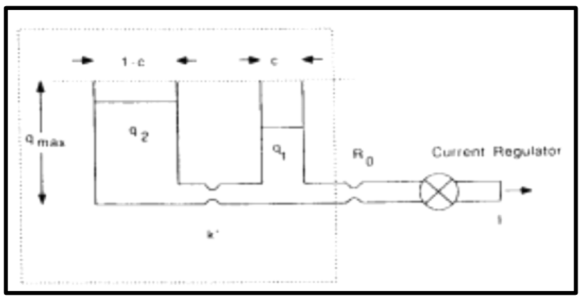

Figure 1.14: Kinetic Battery model
- from (Manwell & McGowan, 1993)

If $q_{1,0}$ and $q_{2,0}$ are taken as the initial amount of charge, the resolution of these equations leads to the equations 1.57 and 1.58.

$$q_2 = q_{1,0}e^{-kt} + \frac{(q_0 kc - I)(1-e^{-kt})}{k} - \frac{Ic(kt-1+e^{-kt})}{k} \tag{1.57}$$

$$q_2 = q_{2,0}e^{-kt} + q_0(1-c)(1-e^{-kt}) - \frac{I(1-c)(kt-1+e^{-kt})}{k} \tag{1.58}$$

where c is the width of the first tank and $1-c$ the width of second tank (Figure 1.14).
The constant $q_{1,0}$, c and k are than to be defined. The proposed resolution process is developed in the APPENDIX B. One can noticed that the temperature effect is not taken into account by this model.

1.3.1.2 CIEMAT model

In the CIEMAT's laboratory, a general battery model for PV system simulation was developpe by (Coppeti, Lorenzo & Chenlo, 1993). Its normalization with respect to the battery capacity allows the generalization of the model to different size of battery. Three types of operating mode are modelled: the discharging mode, the charging mode and the overvoltage mode.

Contrary to KiBaM model, the temperature effect is taken into account. This makes it suitable for regions which go through high temperature during the year.

Thus, the discharge voltage variation with the state of charge SOC is given by the equation 1.59.

$$V_d = [2.085 - 0.12(1 - SOC)] - \frac{I_{bat}}{C_{10}}\left(\frac{4}{1 + I_{bat}^{1.3}} + \frac{0.27}{SOC^{1.5}} + 0.02\right)(1 - 0.007\Delta T) \quad (1.59)$$

where I_{bat} is the discharge current and ΔT the temperature variation regarding the reference temperature 25°C. The depth of discharge DOD is the ratio of the charge Q given by the battery to the battery capacity C at a given time. The state of charge SOC as a complement of DOD is given by the equation 1.60.

$$SOC = 1 - DOD = 1 - \frac{Q}{C} \quad (1.60)$$

The capacity is calculated by the equation 1.61.

$$\frac{C}{C_{10}} = \frac{1.67}{1 + 0.67\left(\frac{I}{I_{10}}\right)^{0.9}}(1 + 0.005\Delta T) \quad (1.61)$$

The equation is normalized with regard to discharge current $I_{bat,10}$ corresponding to the rated capacity C_{10}.

Similarly, the charging voltage is calculated by the equation 1.62.

$$V_c = [2 + 0.16 * SOC] + \frac{I_{bat}}{C_{10}}\left[\frac{6}{1 + I_{bat}^{0.86}} + \frac{0.48}{(1 - SOC)^{1.2}} + 0.036\right][1 - 0.025\Delta \mathrm{T}] \quad (1.62)$$

During the (re)charge, the battery efficiency varies with the state of charge and the charging current. It is obtained with the equation 1.63.

$$\eta_c = 1 - e^{\frac{[\frac{20.73}{\frac{I_{bat}}{I_{bat,10}}+0.55}(SOC-1)]}{}} \quad (1.63)$$

The overcharging phenomenon occurs when the battery continues to be charged after reaching its end charging voltage. It results in gassing evolution that can caused permanent damage. The final charge voltage V_{ec} and the gassing voltage V_g given by the model are function of the charging current. They are traduced by the equation 1.64 and 1.65.

$$V_{ec} = [2.45 + 2.01\ln(1+\frac{I_{bat}}{C_{10}})](1-0.002\Delta T) \quad (1.64)$$

$$V_g = [2.24 + 1.97\ln(1+\frac{I_{bat}}{C_{10}})](1-0.002\Delta T) \quad (1.65)$$

The overcharge voltage phenomenon is represented by an exponential function shown in equation 1.66.

$$V_c = V_g + (V_{ec} - V_g)[1 - e^{\frac{Ah_{restored} - 0.95C}{I_{bat}\tau}}] \quad (1.66)$$

where $Ah_{restored}$ is the ampere-hours stored in the battery during the overcharging. The time constant of the phenomenon τ is given by the equation 1.67.

$$\tau = \frac{17.3}{1 + 852(\frac{I_{bat}}{C_{10}})^{1.67}} \quad (1.67)$$

The same was model used by (Achaibou, Haddadi & Malek, 2012). Two different PV systems were studied. The one equipped with a Varta Solar 100Ah-12V and the other one with a Tudor 800Ah-2V. Simulations results were compared to experimental results. The calculated errors were less than 3% for charging and discharging of the two types of batteries. Compared to KiBaM model, the model of Copetti and al presents a good compromise between complexity and precision. Nevertheless, considering the battery behaviour as a series of steady state could be a simplistic assumption. Reason why, (Guasch and Silvester, 2003) from the electronic engineering department of the Catalan University presented an enhanced model. In this latter, different constants of the Copetti model are taken as variables. In addition, a linear approach is adopted between steady states to avoid discontinuities. Thus, the State of charge and the capacity are given by the equations 1.68, 1.69 and 1.70.

$$SOC(t_i) = \frac{1}{C(t_i)} \int_{-\infty}^{t_i} \eta_i(t) I_{bat}(t) \partial \mathrm{t} \tag{1.68}$$

$$C(t) = \frac{C_{nominal} C_{tcoef}}{1 + A_{cap} (\frac{|I_{bat}(t)|}{I_{nominal}})^{B_{cap}}} (1 + \alpha_c \Delta T(t) + \beta_c \Delta T(t)^2) \tag{1.69}$$

$$I_{nominal} = \frac{C_{nominal}}{n} \tag{1.70}$$

where C_{tcoef}, A_{cap} and B_{cap} the model coefficients, $I_{nominal}$ the discharge current corresponding to $C_{nominal}$ rated capacity, *n* is the time in hours and α_c, β_c the constant coefficients.

1.3.1.3 Personal Simulation Program with Integrated Circuit Emphasis (Pspice) model

A quite different model drawn from simulation made with Pspice was made by (Ameen, Pasupuleti & Khatib, 2015). Pspice is a Personal Simulation Program with Integrated Circuit Emphasis developed by OrCad.

In this model, the charging and the discharging mode are represented. Each of these operating modes is based on the calculation of three parameters: the state of charge, the voltage and the resistance. So, for N_s being the number of 2V series cells, the charging mode is traduced by the equations 1.71, 1.72 and 1.73.

$$SOC(t+\Delta t) = SOC(t)[1-\frac{D}{3600}\Delta t]+\eta_c[V_c I - R_{ch} I^2]dt \quad (1.71)$$

$$V_c = (2+0.148\beta)N_S \quad (1.72)$$

$$R_{ch} = [\frac{0.758+\frac{0.1309}{1.06-\beta}}{SOC_{\mathrm{m}}}]\mathrm{N}_S \quad (1.73)$$

where SOC_m represents the maximum value of the state of charge (equal to 1 in most cases), R_{ch} the charging resistance D the self-discharging rate and β a defined coefficient.
For the discharge, the equations become equations 1.74, 1.75 and 1.76.

$$SOC(t+\Delta t) = SOC(t)[1-\frac{D}{3600}\Delta t]+\eta_c[\frac{V_c I}{3600}]dt \quad (1.74)$$

$$V_d = (1.926+0.124\beta)N_S \quad (1.75)$$

$$R_{disch} = [\frac{0.758+\frac{0.1309}{1.06-\beta}}{SOC_{\mathrm{m}}}]\mathrm{N}_S \quad (1.76)$$

1.4 Inverter

1.4.1 Inverter technology

Inverter or power conditioning unit are used to convert low DC power in high voltage AC. The nominal rated power can go from 50 W to thousands of Watt. In general, inverters are 60% to 95% efficient.

1.4.2 Inverter modelling

1.4.2.1 Single point efficiency

The inverter single point efficiency model (Loutzenhiser, 2001) calculates the AC output power by multiplying the input DC Power with the nominal efficiency of the inverter. This model assumes that the inverter behaviour does not vary under different operating conditions.

1.4.2.2 Sandia inverter performance model

Sandia developed an empirical inverter model (King, Gonzalez, Galbraith & Boyson, 2007). This model has three level of complexity. A simple linear model can be obtained from manufacturer specification sheets. If daylong measurements of the DC power and AC power are available, a parabolic fit (2nd order polynomial) which gives more accuracy to the model is used. The third level of complexity and accuracy is attained with detailed laboratory measurements. In this latter, the power variation due to the voltage is taken into account. Only the simplest form of the model is presented in this review. The maximum AC- power rating given by the manufacturer is noted P_{AC_0}. The corresponding input DC power P_{DC_0} is obtained with the equation 1.77.

$$P_{DC_0} = \frac{P_{AC_0}}{\eta} \tag{1.77}$$

where η is the nominal efficiency of the inverter.

The basic equation of the model is traduced by equation 1.78.

$$P_{AC} = [\frac{P_{AC_0}}{(P_{DC_0} - P_{so})}].[P_{DC} - P_{so}] \tag{1.78}$$

where P_{AC} and P_{DC} respectively the AC power output from the inverter and the DC power input to the inverter. P_{so} is the required DC power to start the inversion process. It is estimate at 1% of the inverter rated power P_{AC_0}.

1.5 System simulation

By the mean of the previous models, the modeling, the simulation and the control strategy of different PV Battery and hybrid system were studied. Some of these studies are presented in this section.

In 2005, (Xu and al., 2005) also work on the sizing of a standalone hybrid wind/PV power system. Batteries were implemented as backup. The excess generated energy is added to this latter and the gap of energy is taken from it. Lanier and Ang model was used for the PV array. The single point efficiency model is used for the inverter. To generate the optimal solution, a genetic algorithm is implemented. In addition to the number of PV array, wind turbines and batteries that might be used, the type of PV module and the optimal tilted angle are given. As application the location of Dagget (California) was chosen. For a load of 2000W, 52x3 PV modules of 50Wp inclined from 59°, 15x24 of 2000 Ah batteries and 10 x1 kW wind turbines were found as optimal solution.

A complete study on photovoltaic system for grid-connected and standalone applications was performed by (Tan and al., 2010). The modelling, control and simulation of the system was performed. The PV array maximum power point is extracted using the five parameters model. A Lithium-Ion battery is used. A 15 kWp power system was chosen for the study.

A performance model of PV-Diesel generator-Battery system was presented by (Ameen, Pasupuleti & Khatib, 2015). A simple efficiency model was used for the PV array. A Pspice model was used for the battery. The diesel generator is used as a backup energy. Load following, and Cycle charging are taken as dispatch strategies. The system consists of a 1.4

kWp PV array, 1kVA DG and an 85 Ah/12V. The validation done with HOMER showed that the proposed model can accurately predict the system's performance.

In 2017, (Shaw and al., 2017) bring out the modeling and the control of a standalone photovoltaic system. A DC-DC boost converter was used to extract the maximum power from the PV array and a bidirectional converter to control the power flow. The modeling was made with a simple model for the array and the Coppeti model for the battery. The inverter was modelled using the single point efficiency model. The PV generator produces 2kW of power and the load was varied from 1.6 kW, 2 kW to 2.4 kW. The solar irradiance was supposed constant. The simulation permitted the validation of the implemented control system.

Despite the interesting conclusions made in these studies, their applications are limited to specific system or location. As an extension to them, several programs and software tools which integrate different components 'model, systems 'topology and data was developed. The most known are presented in the next section.

1.6 Program and Software tools

The National Renewable Energy Laboratory (NREL) has developed a Hybrid Optimisation Model for Electric Renewables (HOMER, 2016). HOMER is suitable to perform the prefeasibility and the optimal sizing of a given hybrid configuration. Various types of technologies and components can be simulated. For PV system, a HDKR model is implemented to estimate solar radiation. After optimization process, the chart of the different feasible configurations is made available. But only Net Present cost minimization is taken into account. Multi objective problems are not be solved. In addition, the PV system is taken as one generic generator. The way modules are coupled is not studied.

The University of Zaragoza developed a quite complete design software tool called iHOGA. iHOGA (Lopez, 2007) means improved Hybrid optimization by Genetic Algorithms. Different types of hybrid systems can be optimized with a mono or multi objective function. Genetic

algorithms are used as research algorithm. To estimate the solar radiation, different model can be chosen: HDKR, Liu and Jordan, Earb, etc. For the batteries, Coppeti and KiBaM models are made available. The optimum slope of the PV panels is evaluated. Contrary to HOMER the LPSP can be fixed at less than 100% of feasibility. This makes it very flexible. In all the studied software, iHOGA is found to be by far the most advanced.

After Hybrid1, the University of Massachusetts developed Hybrid2 (Baring-Gould, 1996) in 1996. It is a Microsoft VISUAL BASIC program software. Hybrid2 contains four parts: the Graphical User Interface (GUI), the simulation Modules, the Economics Module and the Graphical Results Interface (GRI). GUI allows the user to build a project in an organized structure. The simulations are then run in the simulation and economics modules. And the results are finally in GRI.

The Ministry of Natural resources of Canada developed (Retscreen, 1998). It is a feasibility study tool for the evaluation of the cost and the environment impact of a system. On grid and off grid PV system can be studied. Climate database, wind map, hydrology data, PV panels and wind turbines details are made available. Unfortunately, temperature effect on PV modules is not considered. And no optimization process is implemented.

An energy simulation tools named Transient Energy System Simulation Program (Trnsys, 2009) was developed by the University of Wisconsin and Colorado. Trnsys is graphically based software that was initially designed for thermal system. But it was upgraded to simulate photovoltaic, thermal solar and even hybrid system. Optimization process is not implemented.

1.7 Optimisation algorithms

In the two previous paragraphs were cited different software and system simulation which allow an optimization process. To do so, a choice of optimisation algorithm has to be made. Traditional mathematical optimisation algorithm such as Gauss-Newton algorithm and gradient descent method were not found to be efficient enough for such engineering problem

(Saishanmuga Raja and Rajagopalan, 2013). Thus, population-based algorithm have attracted many researchers. Genetic Algorithm, Particle Swarm Optimisation and Ant Colony Optimisation are presented in this chapter.

The Genetic Algorithm is an evolutionary population algorithm. A potential solution to the problem is called “chromosome” which is consist of elements called “genes”. A group of “chromosome” constitute a population. A fitness function is defined to evaluate how each “chromosome” is close to the aimed result. The goal is to make each new generation constitutes with individuals that are closer to the solution than the individuals of the previous generation. The evolution process is made by three steps: ranking, selection and production of new individuals (Saishanmuga and Rajagopalan, 2012). The production of new individuals can be made by a crossover or mutation process. The first one permits the new individuals to inherit “genes” from their parents and the second one allows the individual to randomly change one of its “genes”.

Particle Swarm Optimisation (PSO) (Hansen and al., 2008) is inspired from birds’ movement toward an unknown destination. At the beginning, each bird is flying to a certain direction. After communicating with other birds, all the birds move towards the bird which they supposed to have found the best direction. After that each of them will evaluate its position and then move again towards the bird meant to have the best direction. The same process is repeated till the birds reach the desired destination. At each direction change, the velocity of the birds is also changed.

As for the Ant Colony Optimization (ACO) (Geetha and Srikanth, 2012), the process is based on the fact that ant are able to fine the shortest way from their nets to their food. The space between the nets and the food is made with point. The different points crossed by an ant to go from the nets to the food constitute a path. By laying pheromone in their trail, the more a point is crossed by ants, the more its pheromone intensity increased. The following ant will choose path according to the pheromone intensity. At the end of the process the path recording the higher level of pheromone is chosen as the best solution.

A comparative study (Saishanmuga and al.,2013) of different population-based optimisation algorithm was also performed. Genetic Algorithm was found to be more accurate and less time consuming.

1.8 Synthetis

This wide literature review and summary of fundamental concepts exposed different technology and modelling of different subjects that are linked to PV-battery system design. It goes from the quantification of the solar deposit, PV module, battery and inverter existing technologies and modelling technics, the different software and PV system behaviour prediction tools to finish with optimisation tools. The main goal of this review was to present the different option that could be used to precisely design an optimal energetic photovoltaic system for remote communities.

As for the solar deposit, the HDKR model was chosen as this latter presented a good compromise between simplicity and precision. The review on PV module revealed that the one diode model (or five parameters model) suits best to our need because only manufacturer's data are needed by this latter to give precise result. Despite the analytical approach proposed in KibaM, the fact that the temperature effect is omitted disqualifies it for the current application. Thus, the CIEMAT model is used for the battery. The one-point model is one of the rare inverter models for which only manufacturer's data are needed. This justifies its choice. Regarding the optimisation algorithm, as the comparative studies revealed the different assets of the GA, this latter was chosen to be implemented in the program.

CHAPTER II

OPTIMAL DESIGN OF PV-BATTERY SYSTEM FOR DECENTRALISED ELECTRIFICATION IN SUB-SAHARAN AFRICA

Abdoulaye Sow[1], Daniel R. Rousse[1], Didier Haillot[1,2]

[1]t3e Research Group, Department of Mechanical Engineering, École de Technologie Supérieure, 1100 rue Notre-Dame West, Montréal, Québec, H3C-1K3, Canada

[2]Univ Pau & Pays Adour/ E2S UPPA, Laboratoire de Thermique, Énergétique et Procédés - IPRA, EA1932, 64000, Pau, France.

Paper submitted to Renewable Energy, July 12th 2018

*corresponding author: Daniel R. Rousse

ABSTRACT

While most developing countries have high solar irradiation and thus a potential for solar technology, almost one billion people living in these areas are still in need of electricity. Hence, the purpose of this paper is to present a free access program that ensures accurate and precise design of PV battery systems. It allows price optimization and takes into account market evolution thanks to an embedded database. An innovative two steps algorithm was used to minimize computing resources needed to run the program. It is performed in two steps. A first predesign process based on a coarse sizing method defines the maximum dimensions of the different components of the system. Then, a modelling of the different components allows a dynamic simulation of the system's behaviour with an hour time step, throughout the year. The power management strategy adopted during the simulation allows a refinement of the predesign and an optimisation of the PV battery system designs thanks to genetic algorithm.

Four different infrastructures of the city of ELDORET were used as a case of study. [1]HOMER and [2]iHOGA softwares were used as references to benchmark the proposed tool. This latter permits economies ranging from 9.6% to 36.1% with respect to the coarse design method. In addition, a comparison with grid extension revealed that a decentralised electrification through PV battery systems is by far more cost effective for such low demand. A second comparison with diesel generator confirmed the asset of the PV battery systems in a sustainable development perspective.

Keywords: Decentralized, photovoltaic, optimisation, Sizing, Genetic Algorithms

---

[1] HOMER : Hybrid Optimisation of multiple Energy resource
[2]iHOGA: improved Hybrid Optimisation by Genetic Algorithms
[3] RESCO: Renewable Energy Service Companies
[4]TRNSYS: Transient System simulation tool
[5]NREL: National renewable Energy Laboratory
[6]EPW: Energy Plus Weather file
[7]TMY: Typical Meteorological Year
[8]LPSP: Loss of Power Supply Probability
[9]PSH: Peak Sun Hours
[10]DoDmax: maximal Depth of Discharge
[11]SOC: State of Charge
[12]EPS: Excess of Power Supply
[13]LPS: Loss of Power Supply
[14]HDKR: Hay, Davies, Klutcher and Reindl
[15]KiBaM: Kinetic Battery Model

2.1 Introduction

In 2016, 625 million people were without power in sub-Saharan Africa according to the IEA [1]. That represents 68 percent of the population. Dr. Adesina, the president of the African Development Bank has said: “Africa has energy potential, yes, but we need to unlock that potential. And we must do so quickly, because Africans are tired of being in the dark” [2]. Koffi Annan agreed and argued African governments should “harness every available option, in a cost-effective and a technologically efficient manner as possible, so that everyone is included, and no one is left” [2].

Nowadays, PV panel’s and battery prices have dropped significantly. In addition, the Renewable Energy Service Companies (^{3}RESCO) concept [3] is very suitable for small-scale renewable energy systems. Rather than selling the systems to the homeowners, RESCO sells the service and collects monthly fees in turn. As the company is responsible for maintenance and providing replacement parts, the complexity of the systems for homeowners is no longer a problem. Thus, one can imagine more sophisticated solutions than what is usually implemented. In fact, in new configurations, PV panels and batteries can be connected to a DC bus respectively through a boost converter and a buck-boost converter. With the leasing concept, a power management control strategy is implemented to control the system such that it operates efficiently to minimize power losses and to optimize the cost of the system.

To design such a system, different programs were developed. Eltamaly & Mohamed [4] developed an optimization model to design hybrid renewable energy systems. The main function of this program is to optimize the size of the different components for the lowest price. To use this model, a data bank where all specifications and unit cost of the equipment is required. In parallel, PHOTOV-III [5] has been developed. As the previous one, this program determines the number of PV modules and the capacity of batteries based on load demand. Another program was developed in FORTRAN language to calculate a minimum PV array size for a minimum amount of storage days [6]. In all these tools, very basic models that do

not represent properly the electrical state of the system at each time step were employed to simulate the behaviour of PV panels, batteries and inverters. A more complete model can provide more precise results and thus allow a lower cost for the complete solution that meets a specific need. Furthermore, not all of the above-mentioned programs allow the user to create, enhance and modify a data bank based on local available equipment.

PV.MY [7] was developed for an optimal sizing of PV systems in Malaysia. This software optimizes the size of the different components of a PV system with respect to the electricity needs. It also optimizes the array tilt angle and the inverter size. In addition, it involves the capabilities of predicting the metrological variables such as solar energy, ambient temperature and wind speed using artificial neural networks. But PV.MY is only designed for Malaysia which reduces its diffusion and potential use.

Regarding commercial softwares, four of them can be cited. [4]TRNSYS [8] developed by University of Wisconsin, HYBRID2 [9] and HOMER [10] developed by [5]NREL and iHOGA [11]. TRNSYS was initially developed for thermal systems. It now integrates hybrid systems but doesn't optimize their design. HYDRID2 is specifically created for hybrid systems but doesn't integrate optimisation tools. On the other hand, HOMER optimises hybrid systems and thus can provide PV array power and battery capacity that are needed to satisfy a demand. A choice can also be made among three types of dispatch strategies [12]. But the user must select a type of PV panel, a type of battery and a type of inverter. Hence, a certain level of expertise and experience are needed to use it. The improved Hybrid Optimisation by Genetics Algorithms (iHOGA) [13] optimises different types of hybrid system using Genetic Algorithms. It was developed in C++. The program can choose the optimal types of panel, battery and inverter. It calculates the number of PV panels and the number of batteries of the best configuration. An optimization of the research strategy is done as in HOMER, but it also optimises the state of charge set point. However, most part of these softwares remained relatively expensive, an unlimited free access to them is impossible. In addition, some options

proposed by these tools call for users that have clear notions of electricity, solar deposit evaluation, meteorological data notions, and PV systems knowledge.

This brief review shows that there is a need to bridge the gap between an accurate, precise and optimal design prediction code of PV battery systems and the free availability of a friendly user program. Furthermore, to be use by a huge population it must also be able to run on low computer resources.
The overall aim of this project is then to develop a free access PV-battery system design program to facilitate energy provision in remote areas.

The specific objectives are:

- To implement an innovative PV battery design process;
- To ensure accurate and precise modelling of the different components of the systems;
- To automate some design choices to ease the use of the program;
- To enable cost optimization;
- To make provision to distribute licences freely and allow access to the source-code;
- To implement the formulation in Python language;
- To ensure that all the systems installed in the community have the same components facilitating the ordering process, the maintenance and the resilience of the community.

To present this specific program, the paper has been organized into 6 sections. In section 2, a global description of the program is focussing on essential elements rather than implementation details. The predesign process is exposed in section 3. Section 4 presents in details the heart of the program by showing the different models that were used as well as the developed algorithm. Section 5 describes a case study, exposes its results as well as a comparison with other technologies. Finally, the conclusion is formulated in section 6.

2.2 Program global description

The proposed program will provide, for each studied infrastructure of the community, a unique optimally designed PV-Battery system. Here, all closed enclosures that need to be electrified (houses, school, sanitary, shop…) are considered as infrastructures.

A single DC-bus topology is chosen as system architecture (Figure 2.1). A DC-DC boost converter is used to extract the maximum power from the PV arrays. A DC-DC bidirectional buck boost converter is used to maintain continuous flow between the DC- bus and the batteries with a constant DC-bus voltage. The DC-bus voltage V_{DC-bus} is maintained constant by charging or discharging of the batteries depending on the load change or solar irradiance change.

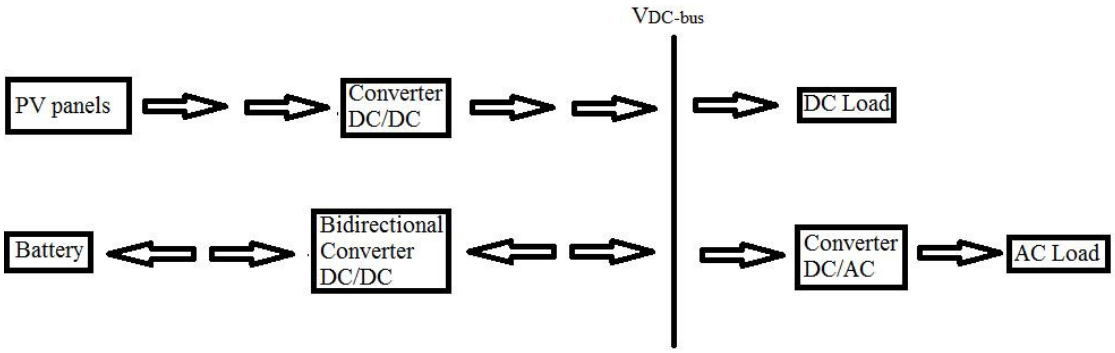

Figure 0.1 : PV-Battery system

Concerning the design process described in Figure 2.2, three input data are required: (1) meteorological data; (2) load data as well as (3) market available components to build the system.

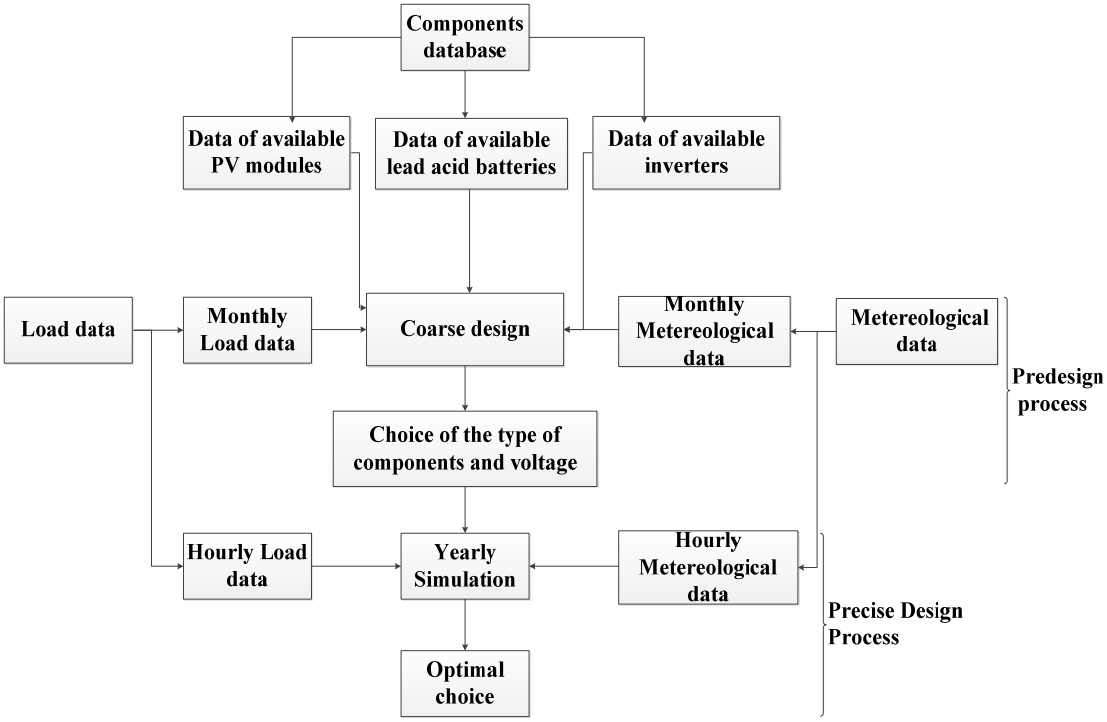

Figure 0.2 : Summarized block diagram of the proposed program

(1) EnergyPlus Weather ([6]EPW) files of the location are used as meteorological data. These latter are synthetized typical meteorological year ([7]TMY) files that are representative of the meteorological condition of the location.

(2) A precise evaluation of the hourly load demand for each studied infrastructure is necessary. Consequently, pre-filled excel datasheets (example in Annex 1) are made available for the user. From this latter, the program directly extracts the hourly consumption of the different infrastructures.

(3) About the system ‘s components, predefined database (Annex 2) containing the specifications of the market available PV panels, batteries and inverters are used. This database can be modified, updated and enhanced by the user.

One novelty of the proposed modelling process is to subdivide the design process in two parts:

1. A predesign process, which includes a coarse design method, is applied first. It is based on monthly meteorological and load data. Three goals are aimed at this first stage: the

choice of one type of PV module, battery and inverter from the database (Annex 2) for the whole community, the sizing of these components for each infrastructure according to the coarse design method and the assignment of an operating voltage for each infrastructure. The chosen operating voltage is imposed as the DC- bus voltage V_{DC-bus} . This process is described in more details in Section 3.

2. The goal of the second step is to optimize the previous sizing of the PV modules and batteries. The whole system is modelled. Yearly simulations are performed based on hourly meteorological data and load data by considering the energy exchange between the different components. For each infrastructure, the optimal number of PV modules and batteries are respectively chosen within the intervals $[0;N_{PV,max}]$ and $[0;N_{bat,max}]$. With $N_{PV,max}$ and$N_{bat,max}$, the number of PV modules and batteries defined in the predesign process. The objective is to find the cheapest system that can ensure a certain level of reliability. The cost index is the Net Present Value (NPV) and the reliability index is the Loss of Power Supply Probability ([8] *LPSP*). The *LPSP* can be defined as the probability that the demand is not satisfied by the power system on a yearly basis. The system must have a *LPSP* inferior to certain reliability threshold ($LPSP_{\max}$) fixed by the user. This process is described in more details in Section 4 where the different parts' modelling are exposed: the PV module, the battery, the inverter, the Plane of Array which allowed the quantification of the amount of energy received by the PV module and the economic part.

As a result, for each studied infrastructure, a PV-Battery system with optimally designed components – is provided by the program. Figure 2.2 provides the gist of the logical structure of the program.

2.3 Predesign process

The predesign process is the first step of the program. As previously mentioned, its objectives are: to fix the operating voltage of the systems, to choose the type of components and to calculate the size of these latter according to a coarse design method. This allows to define oversized systems required by the second step of the program. In the following subsections, the methodology of the predesign is presented first, then the coarse design process is briefly explained.

2.3.1 Predesign methodology

Firstly, the program extracts the consumption of the different infrastructures from Excel's datasheet filled by the user. The total electricity demand of each infrastructure is then calculated by considering the energy lost. Mark and al. [14] evaluated these losses at 20% for DC appliances and 35% for AC appliances.

Then, the DC bus operating voltage must be chosen. Its choice depends on the appliances' voltage and the needed level of power. In remote areas, most part of the appliances works at 12V or 24 V. Labouret and al. [15] suggestion (Table 2.1) was adopted herein.

Table 0.1: System voltage according to its size

Size [Wc]	0-500	500-2000	2000-10000	>10000
Voltage [Vdc]	12	24	48	>48

Only one type of PV module, battery and inverter available in the local market (Annex 2) must be chosen for the whole community to ensure the lowest installation and maintenance costs. To do so, for each PV module of the database (Annex 2), the needed number of panels to satisfy the demand of each infrastructure is determined by use of the coarse design method described next. For each PV module available in the database, the global cost to electrify all the

infrastructures is then calculated. The one presenting the cheapest overall cost is chosen. A similar process is used for the batteries and the inverters.

2.3.2 Coarse design method

The coarse design method is inspired by the work of Mark and al. [14]. It is characterised by its simplicity. PV array as well batteries are sized to satisfy the demand in the worst conditions. All the components are separately sized ignoring the energy exchange between components. Regarding the PV module, the sizing is done for the month of the year with the lowest solar insolation. If I_{MPP} is defined as the maximal power point current given by the PV module manufacturer, the number of PV modules $N_{PV\max}$ is then:

$$N_{PV\max} = \frac{E_T}{I_{MPP} * V_0 * PSH} \tag{2.1}$$

with:

E_T : the yearly energy demand [kWh]

V_0 : the system operating voltage [V]

[9] PSH : the Peak Sun Hours corresponds to an equivalent number of hours during which the instantaneous radiation is supposed to be equal to 1000 W/m^2 .

Regarding the battery, the sizing is made to match the maximum allowable depth of discharge [10] $DOD_{\max}$ and the number of days of storage needed D_R . Mark and al. [14] recommended 50% for the $DOD_{\max}$ and one day for D_R . Hence, the number of batteries $N_{bat\max}$ is given by:

$$N_{bat\max} = INT\left[\frac{E_T * D_R}{C_{bat} * V_0 * DOD_{\max}}\right] + 1 \qquad (2.2)$$

with:

C_{bat} : the capacity of the battery [Ah]

E_T : the yearly energy demand [kWh]

V_0 : the system operating voltage [V]

On the other hand, the inverter is sized according to the level of input power.

2.4 Precise design method

In this section, the coarse design is refined by modelling the different components of the system, simulating the system 's behaviour by adopting a power management strategy and bring out the cheapest system able to satisfy a desired level of demand. An hourly time step Δt is used.

2.4.1 Modelling of the different parts of the system

2.4.1.1 Plane of Array (POA) radiation model

The POA radiation model allows the calculation of the amount of energy received by the PV modules from the sun. The extraterrestrial radiation on a horizontal surface for an hourly period is first calculated. It can be found in classical textbooks such as that of Duffie and Beckman [16]:

$$I_0 = \frac{12*3600}{\pi} G_{sc} \left[1 + 0.033 * \cos\left(\frac{360n}{365} \right) \right] * \left[\cos(\varphi)\cos(\delta)(\sin(\omega_2) - \sin(\omega_1)) + \frac{\pi(\omega_2 - \omega_1)}{180} \sin(\varphi)\sin(\delta) \right] \quad (2.3)$$

where G_{sc} is the solar constant and n the day of the year. ω_1 and ω_2 are the hour angle that defines the considered period. φ and δ respectively correspond to the latitude of the area and its declination. This latter is obtained with:

$$\delta = 23.45 * \sin\left[360\left(\frac{284+n}{365} \right) \right] \quad (2.4)$$

An isotropic diffuse model inspired by Liu and Jordan [17] is used to calculate the solar radiation on tilted surface. It is assumed that the intensity of diffuse sky radiation is considered to be uniform. With a slope angle β and a ground reflectance ρ_g :

$$I_T = I_b R_b + I\rho_g \left[\frac{1-\cos\beta}{2} \right] + I_d \left[\frac{1+\cos\beta}{2} \right] \quad (2.5)$$

I represents the hourly radiation on a horizontal surface. The geometric factor R_b which is the ratio of beam radiation on tilted surface to that of a horizontal surface at any time can be calculated with:

$$R_b = \frac{I_{T,b}}{I_{hor,b}} \approx \frac{\cos\bar{\theta}}{\cos\bar{\theta_z}} \quad (2.6)$$

with $\overline{\theta}$ and $\overline{\theta_z}$ respectively represent surface azimuth and solar azimuth s' average angles. The beam fraction I_b and the diffuse fraction I_d of the radiation are deduced from Earbs and al. [18] correlation. This latter is based on the calculation of the hourly clearness index k_T :

$$k_T = \frac{I}{I_0} \tag{2.7}$$

$$\frac{I_d}{I} = \begin{cases} 1 - 0.09k_T & for\ k_T \le 0.22 \\ 0.9511 - 0.1604 + 4.388k_T^2 - 16.638k_T^3 + 12.336k_T^4 & for\ 0.22 < k_T \le 0.8 \\ 0.165 & for\ k_T > 0.8 \end{cases} \tag{2.8}$$

2.4.1.2 Array performance

Different models are found in the literature but most of them like Sandia's model (King, Boyson & Kratochvill, 2004) require additional information generally not provided by the manufacturer. In this program, the five parameters model is used (Duffie & Beckman, 2014).

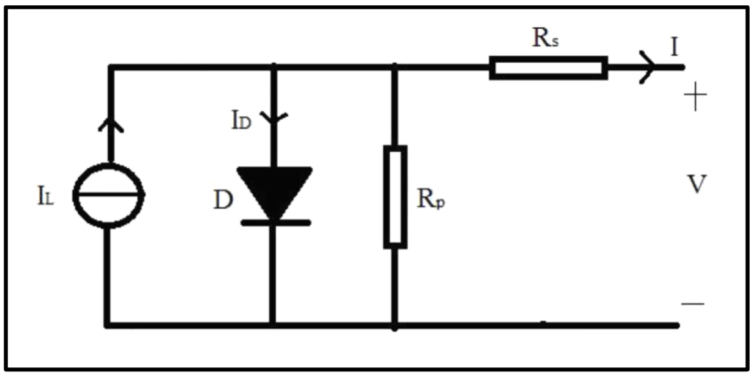

Figure 0.3 : Equivalent circuit of PV generator

Figure 2.3 represents the cell's equivalent circuit used is this model. At fixed solar radiation and temperature, the I-V characteristic given by Duffie & Beckman (2014) is shown by equation 2.9.

$$I = I_L - I_D - I_{sh} = I_L - I_o\left[\exp(\frac{V + IR_s}{a}) - 1\right] - \frac{V + IR_s}{R_{sh}} \quad (2.9)$$

where the light current I_L, the diode reverse saturation current I_o, the series resistance R_s, the shunt resistance R_{sh} and the parameter a, are the five parameter to be determined. To do so, five different conditions are used by Duffie & Beckman, (2014). Three of them are taken from manufacturer's information.

At short circuit conditions, the voltage is zero, the current is $I_{sc,ref}$ is given by equation 2.10.

$$I_{sc,ref} = I_{L,ref} - I_{o,ref}\left[\exp\left(\frac{I_{sc,ref}R_{s,ref}}{a_{ef}}\right) - 1\right] - \frac{I_{sc,ref}R_{s,ref}}{R_{sh,ref}} \quad (2.10)$$

The current is zero at open circuit conditions and the voltage is $V_{oc,ref}$:

$$I_{L,ref} = I_{o,ref}\left[\exp\left(\frac{V_{oc,ref}}{a_{ref}}\right) - 1\right] + \frac{V_{oc,ref}}{R_{sh,ref}} \quad (2.11)$$

At the maximum power point, the model gives the equation 2.12.

$$I_{mp,ref} = I_{L,ref} - I_{o,ref}\left[\exp(\frac{V_{mp,ref} + I_{mp,ref}R_{s,ref}}{a_{ref}}) - 1\right] - \frac{V_{mp,ref} + I_{mp,ref}R_{s,ref}}{R_{sh,ref}} \quad (2.12)$$

with $I_{\mathrm{mp},ref}$ the current, and $V_{\mathrm{mp},ref}$ the voltage.

The fourth condition is a result of the fact that the derivative of the power with respect to the voltage is equal to zero. It gives equation 2.13.

$$\frac{I_{mp,ref}}{V_{mp,ref}} = \frac{\frac{I_{o,ref}}{a_{ref}} \exp\left[\frac{V_{mp,ref} + I_{mp,ref} R_{s,ref}}{a_{ef}}\right] + \frac{1}{R_{sh,ref}}}{1 + \frac{I_{o,ref} R_{s,ref}}{a_{ref}} \exp\left[\frac{V_{mp,ref} + I_{mp,ref} R_{s,ref}}{a_{ref}}\right] + \frac{R_{s,ref}}{R_{sh,ref}}} \tag{2.13}$$

For the fifth condition, the temperature coefficient of open circuit voltage $\mu_{V_{oc}}$ is used to calculate V_{oc} at a different temperature. It is done through equation 2.14.

$$V_{oc}(T_c) = V_{oc}(T_{c,ref}) + \mu_{V_{oc}}(T_c - T_{c,ref}) \tag{2.14}$$

Numerical means are used to solve this system of equation. The solution provides the current and the voltage at the output of the PV generator at the reference conditions (I=1000 W/m^2, T=25°C). To complete the model, following equations (Duffie & Beckman, 2004) are used to determine parameters values according to the variation of the solar radiation and the temperature. Equations 2.15-2.20 are used.

$$I_L = \frac{S}{S_{ref}}\left[I_{L,ref} + \mu_{I_{sc}}(T_c - T_{c,ref})\right] \tag{2.15}$$

$$I_o = I_{o,ref}\left[\left(\frac{T_c}{T_{c,ref}}\right)^3 \exp\left(\frac{E_g}{kT}\bigg|_{T_{c,ref}} - \frac{E_g}{kT}\bigg|_{T_c}\right)\right] \tag{2.16}$$

$$E_g = E_{g,ref}\left[1 - C(T - T_{c,ref})\right] \tag{2.17}$$

$$R_s = R_{s,ref} \tag{2.18}$$

$$R_{sh} = R_{sh,\mathrm{ref}} \frac{S_{ref}}{S} \tag{2.19}$$

$$a = a_{ref} \frac{T_c}{T_{c,ref}} \tag{2.20}$$

with $E_{g,ref} = 1.12\,eV$ and $C = 0.0002677$

In summary, equations (2.10) through (2.14) are solved to determine the five parameters at the reference conditions, and equations (2.15) and (2.20) are used to adapt them to real condition of use. This latter are then used to adapt the equation (2.13) to real condition. Then, equations (2.13) and (2.21) which is the general I-V equation at the maximum point are used to calculate the maximum power.

$$I_{mp} = I_L - I_o \left[\exp\left(\frac{V_{mp} + I_{mp} R_s}{a} \right) - 1 \right] - \left[\frac{V_{mp} + I_{mp} R_s}{R_{sh}} \right] \tag{2.21}$$

The maximum power produced by the PV module is given by equation 2.22.

$$P_{PV} = I_{mp} * V_{mp} \tag{2.22}$$

So the energy E_{PV} generated by a PV array constituted of N_{PV} modules during a time step Δt is given by equation 2.23.

$$E_{PV} = N_{PV} P_{PV} \Delta t \tag{2.23}$$

2.4.1.3 Battery model

Battery modelling is capital for simulation of a standalone system. Many parameters vary during a battery operation: voltage, current, density, temperature, resistivity, etc, making its modelling complicated. For this reason, many models can be found in the literature. The model elaborated at CIEMAT laboratory by Copetti and al. (1993) is adopted in this program. It is specific to PV systems simulation. The normalization of its equations made it accurate to represent several lead acid batteries. Furthermore, only inputs from manufacturers are required. Copetti and al. (1993) propose the state of charge SOC and the voltage as the two main indicators of the battery's behaviour.

The amount of energy exchanged by the battery with the rest of the system is given by equation 2.24.

$$E(t) = \left(\frac{P_{PV}(t) - P_{Load}(t)}{\eta_{conv\_bid}} \right) \Delta t = \frac{E_{PV}(t) - E_{load}(t)}{\eta_{conv\_bid}} \tag{2.24}$$

with E_{PV} and E_{load} respectively the energy generates by PV modules and the energy demand. This energy exchange might be negative for a discharge and positive for a charge. In a charging case, Copetti and al. (1993) propose the calculation of the battery stored energy E_{bat}, the state of charge SOC, the efficiency η_c and the capacity C with the following equations:

$$E_{bat}(t) = E_{bat}(t-1) + \eta_c(t)E(t) = E_{bat}(t-1) + \frac{\eta_c(t)[E_{PV}(t) - E_{load}(t)]}{\eta_{conv\_bid}} \tag{2.25}$$

$$SOC(t) = SOC(t-1) + \frac{\eta_c(t)Q(t)}{C(t)} \tag{2.26}$$

$$Q(t) = \frac{E(t)}{V(t)} \tag{2.27}$$

$$V_c(t) = \frac{I(t)}{C_{10}}\left[\frac{6}{1+I(\mathrm{t})^{0.86}} + \frac{0.48}{(1-SOC(t))^{1.2}} + 0.036\right] * \left(1 - 0.025\Delta \mathrm{T}\right) + \left[2 + 0.16 * SOC(t)\right] \tag{2.28}$$

$$\eta_c(\mathrm{t}) = 1 - \exp\left[\left(\frac{20.73}{\frac{I(t)}{I_{10}} + 0.55}\right)(SOC(t) - 1)\right] \tag{2.29}$$

$$\frac{C(t)}{C_{10}} = \left[(1 + 0.005\Delta T)\frac{1.67}{1 + 0.67(I(t)/I_{10})^{0.9}}\right] \tag{2.30}$$

$$\Delta T = T(t) - T_{ref} \tag{2.31}$$

with T_{ref} =25°C

For the discharge case Copetti and al. (1993) propose the following equations.

$$E_{bat}(t) = E_{bat}(t-1) + \eta_c(t)E(t) = E_{bat}(t-1) + \frac{E_{PV}(t) - E_{load}(t)}{\eta_{conv\_bid}} \tag{2.32}$$

$$SOC(t) = SOC(t-1) + \frac{Q(t)}{C(t)} \tag{2.33}$$

$$Q(t) = \frac{E(t)}{V(t)} \tag{2.34}$$

$$V_d(t) = \left[2.085 - 0.12(1 - SOC(t))\right] - \frac{I(t)}{C_{10}}\left[\frac{4}{1+I(t)^{1.3}} + \frac{0.27}{SOC(t)^{1.5}} + 0.02\right]\left(1 - 0.007\Delta T\right) \tag{2.35}$$

$$\eta_d(\mathrm{t}) = 1 \tag{2.36}$$

2.4.1.4 Inverter model

In the literature, the inverter is mostly modelled by using the nominal efficiency given by the manufacturer. But when the P_{AC} is very low compared to the rated AC-power P_{AC_0}, the efficiency of the inverter decreases. To take this phenomenon into account, Sandia developed an empirical or phenomenological model (King, Gonzalez, Galbraith & Boyson, 2007). The rated AC-power P_{AC_0} and the nominal efficiency η_{inv_0} are given by the manufacturer. Dividing P_{AC_0} by the efficiency value provides a value for the associated DC-power level P_{DC_0} .The DC-power required to start the inversion process P_{s_0} is estimated at 1% of the inverter's rated power. So for each call of AC-power P_{AC}, the system has to generate the following DC-power P_{DC}:

$$P_{DC} = P_{s_0} + \left[\frac{P_{DC_0} - P_{s_0}}{P_{AC_0}} \right] P_{AC} \tag{2.37}$$

2.4.1.5 Converters

In the suggested program, converters are solely modelled according to their efficiency.

2.4.2 Economic model

Three types of expenses are taken into account in the economic model. The initial capital cost C_i, the present value of the operation and maintenance cost C_{OM} and the present value of replacement cost C_R . The Net Present Value NPV is then:

$$NPV = C_i + C_{OM} + C_R \tag{2.38}$$

The initial capital cost C_i is given by:

$$C_i = N_{PV} * C_{PV} + N_{Batt} * C_{Batt} + C_{inv} + C_{Conv} + C_{conv-bid} \quad (2.39)$$

where N_{PV} and N_{Batt} are the number of PV modules and the number of batteries, respectively. And $C_{PV}, C_{Batt}, C_{inv}, C_{conv-bid}$, C_{conv} are the unit price cost of the PV module, the unit price cost of the battery, the price of the inverter, the price of the bidirectional converter and the price of the boost converter, respectively. The program extracts these costs directly from the embedded database. The lifetimes T_{rep} of the converters, the batteries and the inverter are fixed. The installation will last as long as T. Considering an inflation rate i, the present value of the replacement cost C_R is:

$$C_R = \sum_{j=1}^{N_{rep}} (\mathrm{N}_{Batt} * \mathrm{C}_{Batt} + \mathrm{C}_{inv} + C_{conv} + \mathrm{C}_{con\_bid})(1+\mathrm{i})^{T_{rep} \cdot j} \quad (2.40)$$

where $N_{rep} = \frac{T}{T_{rep}}$ is the number of replacements.

C_{OM} is given by:

$$C_{OM} = \sum_{j=1}^{T} 1\% * C_i * (1+i)^j \quad (2.41)$$

2.4.3 LPSP definition

The Loss of power Supply Probability (*LPSP*) is used to evaluate the probability of the system to not satisfy the whole demand. It is evaluated through a power management strategy described in Figure 2.4. It is defined by:

$$LPSP = \frac{\sum_{t=1}^{8760} LPS(t)}{\sum_{t=1}^{8760} E_{load}(\mathrm{t})} \tag{2.42}$$

with LPS the Loss of Power Supply. It is the unsatisfied amount of energy at each hour of the year. When the amount of energy exceeds the need, the Excess of Power Supply Probability is calculated as:

$$EPSP = \frac{\sum_{t=1}^{8760} EPS(t)}{\sum_{t=1}^{8760} E_{load}(\mathrm{t})} \tag{2.43}$$

with EPS the Excess of Power Supply. It is the excess amount of energy at each hour of the year.

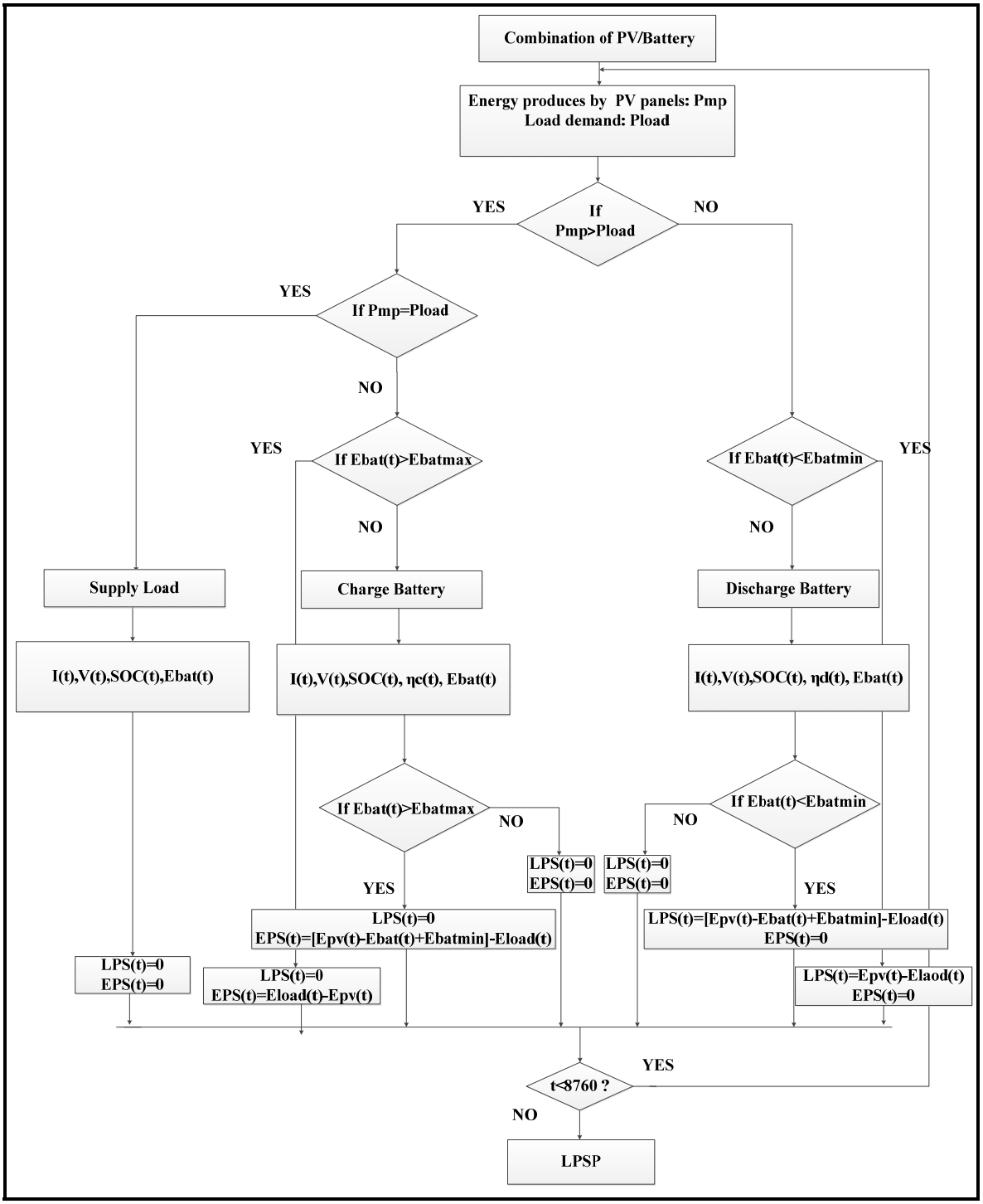

Figure 0.4 : Evaluation of the Loss of power Supply Probability *(LPSP)*

The power management strategy used in this program is basic. Seven main operating modes are noticed during this energy balance. When the generated power exceeds the power load, the Loss of Power Supply is equal to zero. At this stage, three scenarios are possible: (1) the batteries are fully charged and the excess energy is dissipated through the dump load; (2) the batteries are not fully charged and the excess energy is stored in the batteries but the maximal storable energy $E_{bat\max}$ is reached; and finally (3) the batteries are not fully charged and the excess energy is stored in the batteries without reaching $E_{bat\max}$. In these three different cases, the Excess of Power Supply becomes:

$$EPS(t) = \begin{cases} E_{PV}(t) - E_{load}(t) & (1) \\ E_{PV}(t) + E_{bat\max} - E_{bat}(t-1) - E_{load}(t) & (2) \\ 0 & (3) \end{cases} \qquad (2.44)$$

Otherwise, when the PV module doesn't generate enough power, the Excess Power of Supply is equal to zero. And three others scenarios can be noticed: (1) the batteries are fully discharged and the demand is not satisfied (2) the batteries are not fully discharge and the lack is fulfilled by the batteries but the minimal level of energy $E_{bat\min}$ is reached and finally (3) the batteries are not fully discharge and the lack is fulfilled by the batteries without reaching $E_{bat\min}$. In these three different cases, the Loss of Power Supply becomes:

$$LPS(t) = \begin{cases} E_{load}(t) - E_{PV}(t) & (1) \\ E_{load}(t) - [E_{PV}(t) + E_{bat}(t-1) - E_{bat\min}] & (2) \\ 0 & (3) \end{cases} \qquad (2.45)$$

One last scenario is when the PV modules generation is equal to the load. In that case, $LPS = EPS = 0$. The batteries are neither charged nor discharged.

One can notice that for each charge or discharge of the batteries, different parameters as $I(t), V(t), SOC(t), \eta(t)$ are evaluated using the equations exposed in Section 3.

This process is repeated for the 8760 hours of the year. So, the $LPSP$ is evaluated for each system.

2.4.4 Genetic Algorithm and numerical resolution

2.4.4.1 Genetic algorithm

Genetic Algorithm is a search method that imitates the biological evolution. It provides an easy way to come up with quick and feasible solution. All that is needed is to define the individuals, the fitness function and constraints, the population size, the number of generation and genetic operators.

- The individuals: are represented by the combination of PV modules and batteries $[N_{PV}; N_{bat}]$. A group of individuals forms the population.
- The fitness function is the individual s' characteristic to be evaluated. The individuals are ranked according to this function. In this program, the fitness function is the cost (Equation 2.40). A certain level of reliability defines by $LPSP_{\max}$ is imposed as a constraint.
- The population size N_p and the number of generations $N_{gen\max}$ have to be chosen to help to reach the best solution in a relatively short time. These two parameters have to be determined after several tests to find the good regulation. A good population size was found to be equal to $\max(N_{PV\max}; N_{bat\max})$. Thus, the research space can be adapted to the size of the system. The number of generations was fixed at 15.
- The genetic operators that were used are: the crossover, the mutation and the selection. The crossover operator is used to form two chromosomes (children) from two others

(parents). It takes place according to a certain probability which is fixed at 0.5 [22] in the program. The mutation operator is a random modification of the chromosome according to a certain probability which is fixed at 0.1 in the program. This latter helps the program to avoid converging too soon to local solution. Regarding the selection, it is the choice of the chromosomes that will produce the next generation through the crossover and the mutation process. In this program, the 50% better chromosomes are chosen.

Figure 2.5 describes the genetic algorithm process used in the program. An initial generation is randomly produced. The cheapest of these combinations from those that have a $LPSP$ inferior to the $LPSP_{\max}$ previously entered by the user is chosen as the optimal solution. From the rest are selected the 50% better which will go through the crossing and the mutation process. So is formed the new generation. The individuals of this generation are in their turn evaluated. And the best individual among them that respect the constraint is compared to the optimal solution retained previously. The cheaper of the two is chosen as the new optimal solution. And this process is repeated until the number of generations $N_{gen\ max}$ is reached (Figure 2.5).

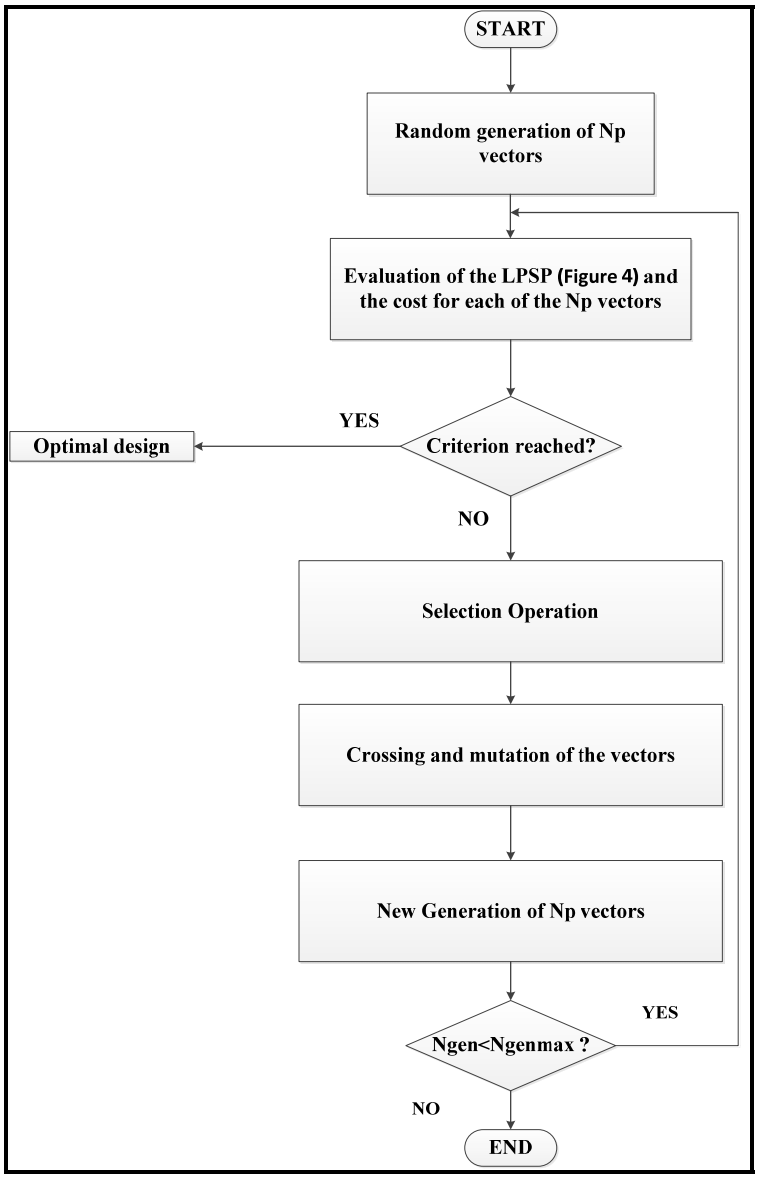

Figure 0.5 : Genetic algorithm process used in the program

2.4.4.2 Numerical method

For the dynamic simulations, two equation systems have to be solved several times. The first one is the PV module s' five parameters model (Equation 2.10-2.14). And the second one is the CIEMAT model that is equations 2.26 to 2.30 for the charging or equations 2.33 to 2.37

for the discharging. The two are systems of five implicit equations with five unknowns. These systems are solved using a python ‘s tool named “root” which is suitable to solve equations with vector functions [23]. An hourly time step is adopted.

The computer is an Intel core 3.6GHz, 32 Go RAM, with Windows 7 operating system. The program is implemented in Python. The simulation time was estimated at 3h to 4h.

2.5 Case study

2.5.1 Eldoret, Kenya

PV-Battery systems were optimally designed for four infrastructures of the city of Eldoret, Kenya (0° 31’ North,31° 17’ East): a house, some floor lamps, a school and a health centre. The infrastructure appliances are presented in Annex 1 and the daily load profiles are illustrated in Figure 2.6 as constant sequence of power for 1h time-steps. The AC loads, and DC loads respectively correspond to the power demand of AC appliances and DC appliances. The hourly EnergyPlus Weather (EPW) file of Eldoret is used by the program. The Global solar irradiation and the ambient temperature of the first of January was extracted from that file and is shown as an example in (Figure 2.7).

Different types of components were taken into account (Annex 2): twelve types of PV modules, eleven types of batteries and eight types of inverters. The minimum state of charge of the batteries is fixed at 40%. The PV arrays are inclined at angle equal to latitude. A full satisfaction of the load is targeted i.e. $LPSP_{\max} = 0$.

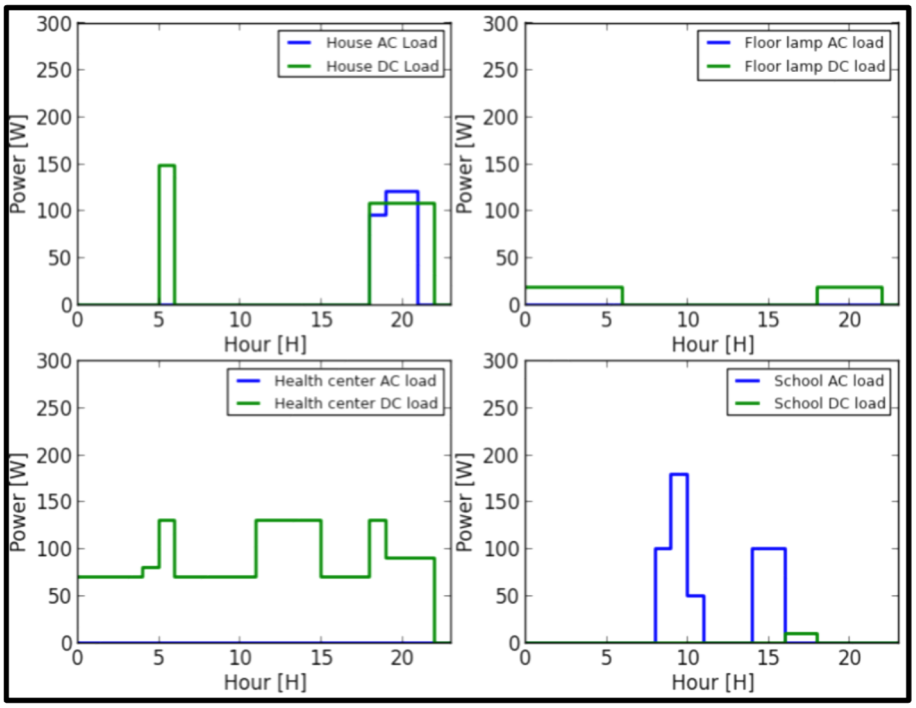

Figure 0.6 : Hourly Consumptions of the different infrastructures

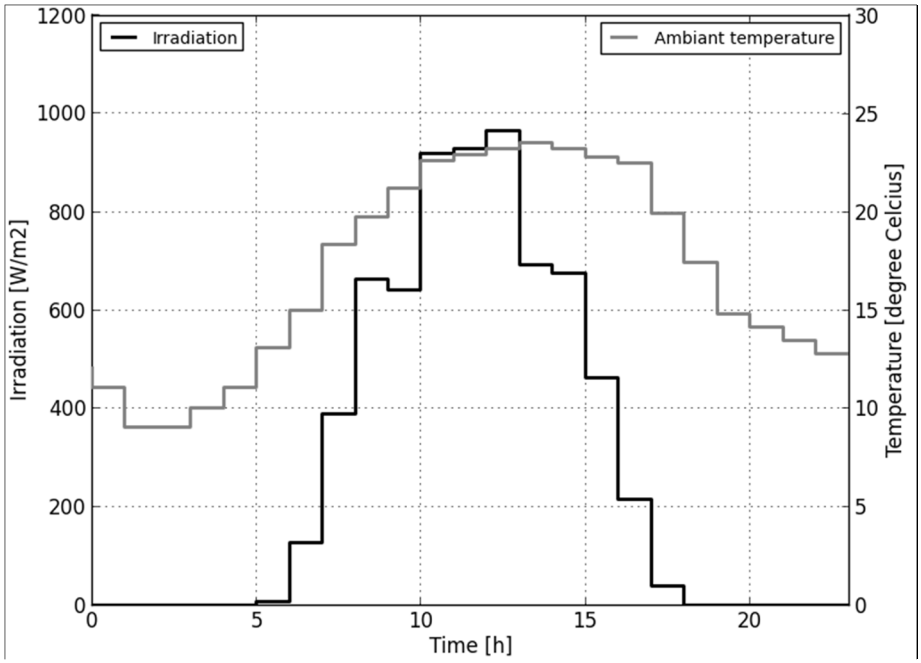

Figure 0.7 : Hourly Meteorological data
on the first of January in Eldoret

2.5.2 Validation

For the four infrastructures, among the different systems presented in Annex 2, the SLP120 polycrystalline of 120Wc and the battery UPG UB12500 AGM of 90 Ah were chosen by the program. An operating voltage of 12V was attributed to the house, the floor lamps and the school. While a 24V system was chosen for the health center as a fridge of 24V is needed (Annex 1). For each system, a corresponding inverter was attributed. A Cotek S150 112 was proposed 12V systems and a Cotek S150 124 for the health center.

Tables 2.2-2.6 present the design results for the four infrastructures, respectively. These tables compare the program results to those obtained with the coarse design method and those predicted by iHOGA and HOMER softwares. As outputs, tables 2.2-2.6 present the peak power of PV, the nominal capacity of batteries, the unmet load, the annual battery throughput, the annual energy delivered by PV and the annual overload energy.

Table 0.2: Comparison between different methods (House Load, VDC=12V)

	Coarse-design	Program	HOMER	iHOGA
Peak Power of PV panels (kW)	0.36(1x3panels of 120W,12V)	0.36(1x3panels of 120W,12V)	0.36(1x3panels of 120W,12V)	0.36(1x3panels of 120W,12V)
Nominal Capacity of batteries (kWh)	6.48(1x6 batteries of 90 Ah, 12V)	4.32(1x4 batteries of 90 Ah, 12V)	5,4(1x5 batteries of 90 Ah, 12V)	4.32(1x4 batteries of 90 Ah, 12V)
Unmet Load (%)	0	0	0	0
Annual battery throughput	-	350.58	393	375
Annual Energy delivered by PV generator (kWh/yr)	-	578.63	774	587
Annual overall load energy (kWh/yr)	333	333	333	333

Table 0.3: Comparison between different methods (Floor Lamp Load, VDC=12V)

	Coarse-design	Program	HOMER	iHOGA
Peak Power of PV panels (kW)	0.12(1x1panels of 120W,12V)	0.12(1x1panels of 120W,12V)	0.12(1x1panels of 120W,12V)	0.12(1x1panels of 120W,12V)
Nominal Capacity of batteries (kWh)	2.16(1x2 batteries of 90 Ah, 12V)	1.08(1x1 batteries of 90 Ah, 12V)	1.08(1x1 batteries of 90 Ah, 12V)	1.08(1x1 batteries of 90 Ah, 12V)
Unmet Load (%)	0	0	0	0
Annual battery throughput	-	71.77	72.2	78
Annual Energy delivered by PV generator (kWh/yr)	-	192.87	258	195
Annual overall load energy (kWh/yr)	72	72	72	72

Table 0.4: Comparison between different methods (School Load, VDC=12V)

	Coarse-design	Program	HOMER	iHOGA
Peak Power of PV panels (kW)	0.24(1x2panels of 120W,12V)	0.24(1x2panels of 120W,12V)	0.24(1x2panels of 120W,12V)	0.24(1x2panels of 120W,12V)
Nominal Capacity of batteries (kWh)	4.32(1x4 batteries of 90 Ah, 12V)	1.08(1x1 batteries of 90 Ah, 12V)	1.08(1x1 batteries of 90 Ah, 12V)	1.08(1x1 batteries of 90 Ah, 12V)
Unmet Load (%)	0	0	0	0
Annual battery throughput	-	58.083	56.9	57
Annual Energy delivered by PV generator (kWh/yr)	-	385.75	519	391
Annual overall load energy (kWh/yr)	200	200	200	200

Table 0.5: Comparison between different methods (Health center, VDC=24V)

	Coarse-design	Program	HOMER	iHOGA
Peak Power of PV panels (kW)	0.72(2x3panels of 120W,12V)	0.72(2x3panels of 120W,12V)	0.72(2x3panels of 120W,12V)	0.72(2x3panels of 120W,12V)
Nominal Capacity of batteries (kWh)	12.96(2x6 batteries of 90 Ah, 12V)	6.48(2x3 batteries of 90 Ah, 12V)	6.48(2x3 batteries of 90 Ah, 12V)	6.48(2x3 batteries of 90 Ah, 12V)
Unmet Load (%)	0	0	0	0
Annual battery throughput	-	406.38	416	457
Annual Energy delivered by PV generator (kWh/yr)		1157.26	1438	1174
Annual overall load energy (kWh/yr)		781	781	781

The first level of comparison concerned the first two lines of the tables which represent the peak power of PV and the capacity of batteries. Regarding these outputs, the results obtained by the program were very similar to those obtained by iHOGA and HOMER. In fact, with one exception, the three programs propose, as optimal solution, the same number of PV modules and batteries. HOMER proposes for the house a solution with one more battery. This difference can be associated to the modelling differences between the programs. Modelling differences that appear clearly with the consideration of the other outputs: the annual battery throughput, the annual energy delivered by PV.

About these latter the comparison with iHOGA revealed that the PV annual delivered energy calculated by this commercial program is slightly more important than the one calculated by the proposed one. The differences are in the order of 1.4% for the house, 1.1% for the floor lamp, 1.3% for the school and 1.4% for the health center. These slight differences confirm the similarity of the solutions proposed by iHOGA to those by the program. Furthermore, these differences can be associated to the modelling difference. In fact, in iHOGA, the generated power is calculated by multiplying the voltage with the short circuit current of the module and the irradiance. Such method is different from the five parameters model used in the proposed

program. This modelling difference introduces more discrepancy in battery energy throughput calculations. A maximum discrepancy of 12% is reached for the 24V system. A detailed explanation for this difference cannot be provided as the battery model used in iHOGA is not exposed in its user's manual. But as for the PV module, a battery modelling difference is expected to be the cause. Despite this energy calculation difference, the solution found by the program is in all cases similar to the one found by iHOGA in terms of component requirements. Hence, according to this first validation, the proposed program is considered to accurately model and design PV-Battery systems.

Regarding the comparison with HOMER, higher differences were obtained. In fact, the PV generated energy calculated by HOMER is greater than the one calculated by the program and iHOGA. Comparing the program with HOMER is more difficult as this latter presents very different modelling with respect to the other two programs. Regarding the plane of array modelling, the [14]HDKR [24] model was implemented in HOMER contrary to the isotropic model of the program. Concerning the PV energy, HOMER calculates the PV array output power by multiplying the nominal power output of a generic PV generator with the ratio of global solar radiation on real condition and global solar radiation on standard condition (1000 W/m^2). The temperature coefficient of power is used for the temperature influence. In addition, a derating factor is used to account for reduced output in real word operating condition. This is quite far from the five parameters model used by the program. Despite these modelling differences, the results for the battery throughput between HOMER and the program were found to be quite close. 10% more energy throughput was noticed for the house as for this latter one more battery is proposed by HOMER. Furthermore, when it comes to battery requirements, the [15]KiBaM [25] model is used by HOMER for the battery modelling instead of the CIEMAT model. Despite this difference, the discrepancy is still reasonable.

This second comparison showed that despite different modelling strategies embedded in HOMER and the program – difference clearly appears in the PV energy calculation – the

overall solutions proposed by the two programs were similar. In fact, only for the house system (Table 2.3), HOMER calculates one more battery.
Overall, the above-described comparisons showed that the proposed program is suitable for modelling and designing PV battery systems.

Regarding the coarse design, the number of PV module found by this latter is like the one found by the program. That is not the case for the battery. This might be due to the fact that the coarse design process fixes a certain number of days of autonomy which oversized the system. It has economic consequences that are bring to light in next chapters.

2.5.3 System behaviour

To analyse the designed behaviour of the system, the case of the PV-Battery system for the house is used. Figure 2.8 presents the hourly consumption, the generated PV power and battery throughput energy during the first three days of January. Initially, the batteries are supposed to be fully charged. To facilitate comprehension, the energy taken from the battery is counted negative and the energy put into the battery is counted positive.

The batteries discharge starts at 6h in the morning before sunrise and is pursued from 18h to 22h when the peak demand occurs. Figure 2.8 also shows that the PV array charges the batteries after sunrise until sunset (18h). The first recharge process occurs with a very low efficiency, due to the relatively high state of charge of the battery as shown by the equation 36. The battery is then discharged during the night which decreases the state of charge. Thus, the charge process on the second day begins with a very high efficiency; almost 100%. After reaching a certain state of charge, the charging rate decreases with the energy level that is less energy is accepted by the battery until achieving the maximum allowable energy level. At this point, no more energy is accepted in the battery. The same process is repeated on the third day.

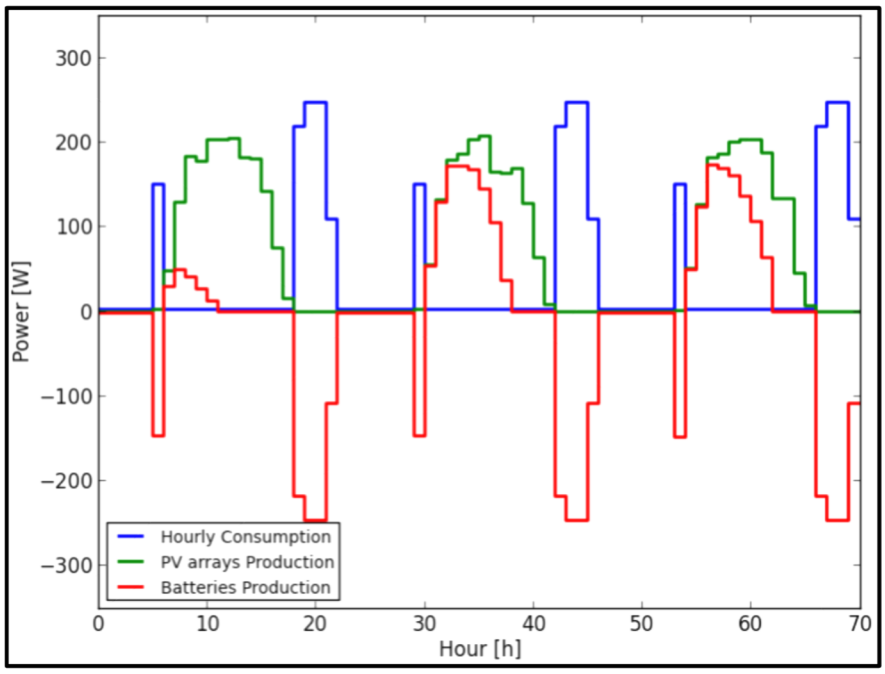

Figure 0.8 : The home PV-Battery system
behaviour during the three first days of the January

The same dynamic analysis is carried out for the other three systems (figure 2.9-2.11). Depending on the hourly consumption profile, the system's behaviour can be more or less difficult to understand. One can notice that during these three days of operation, a relatively important amount of energy is lost. For the house (figure 2.8), the flour lamps (figure 2.9), the school (figure 2.10) and the health center (figure 2.11) the percentage of lost energy during the year are respectively: 23.7%, 9.7%, 4.6% and 10.4%. These percentages of loss are directly linked to the consumption profiles. For the house, the system is essentially used during the evening. The same behaviour is noticed for the Lamp on a smaller scale. The reverse phenomenon appears for the school. The system is more solicited during the day. Reason why, the battery is almost always full. Thus, the excess power produce during the day can't be stored in the battery. The School's consumption profile is the most balanced. The reason why its system has the smallest loss. So, the repartition of consumption throughout the day is very important. A well-shared consumption can help to reduce the system's size and also avoid power loss. Thus, population has to be sensitized about the importance of having a well-shared

consumption throughout the day. This educative aspect is very often neglected. Reason why lot of rural electrification project find problem of sustainable.

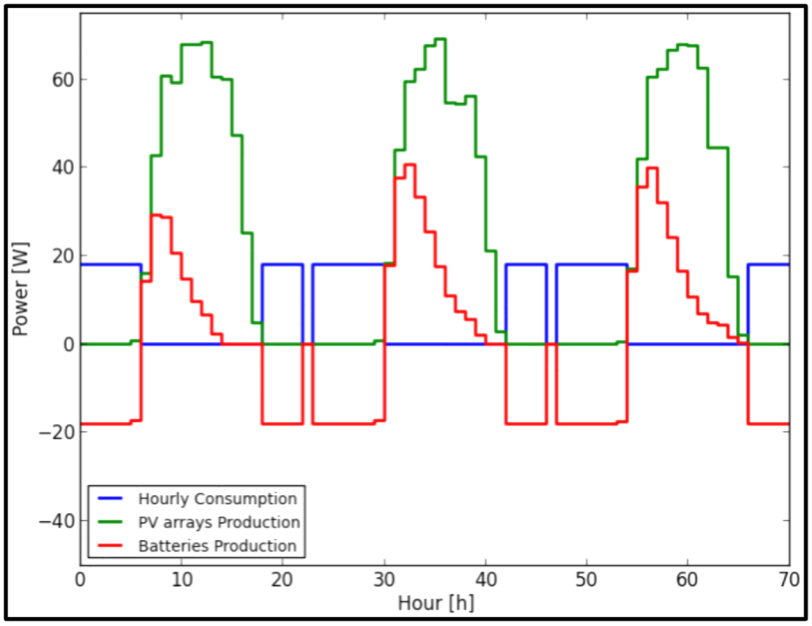

Figure 0.9 : Floor lamps' PV-Battery System Behaviour during three first days of January

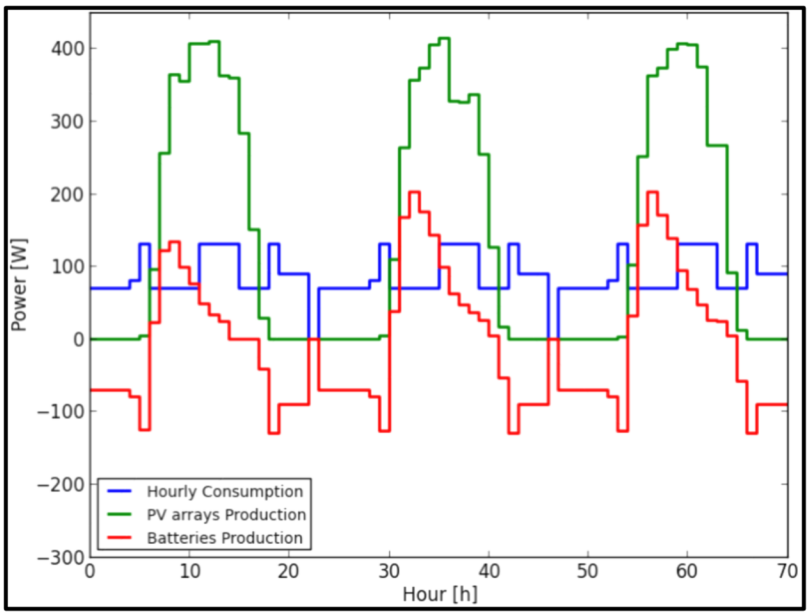

Figure 0.10 : School's PV-Battery System Behaviour during three first days of January

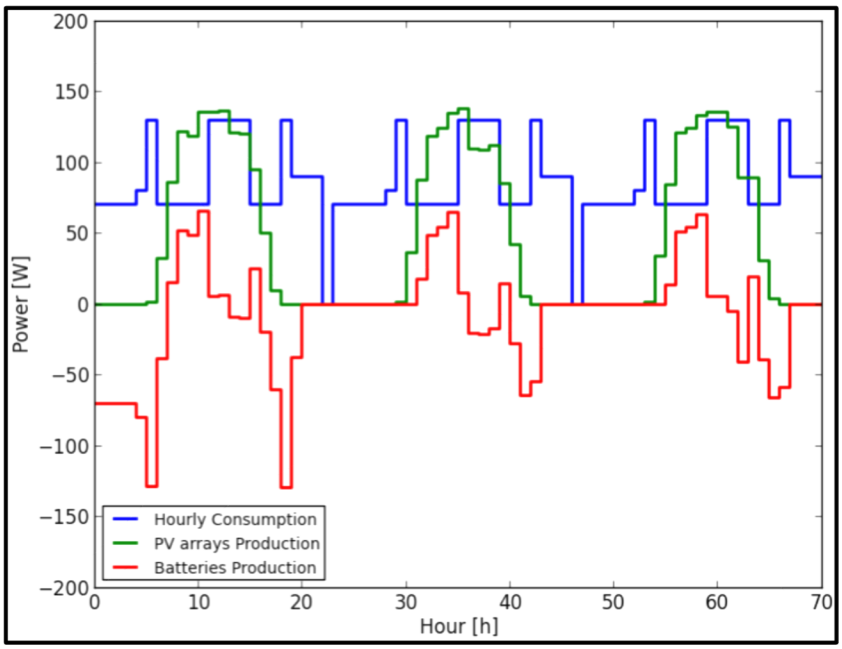

Figure 0.11 : Health Care's PV-Battery System Behaviour during three first days of January

2.5.4 Economic considerations

To show the economical advantages of using this program, a comparison was made with the coarse design. The unity price of the PV module is 269.7$, the unity price of the chosen battery is 103$. The inverter cost 149$. A converter price is estimated at 50$ [26]. The lifetime of the batteries, the converters and the inverters are fixed to 5 years. The installation is supposed to last 20 years. The comparison, presented in Figure 2.12, revealed that a profit from 9% to 38% can be made by using the program. This is mainly due to the control strategy that helps to designed systems that shaped the best the population need.

Table 0.6Table: Economic savings resulting from the Program

	House	Floor Lamp	School	Health Center
Coarse design	4013.52	1635.84	2824.68	7580.04
Program designed system	3253.1	1477.7	1747.4	4886.2

% economy	18.9	9.6	38.1	35.5

2.5.5 Optimal $LPSP_{max}$

As explained in a previous chapter, in program, the value of $LPSP_{\max}$ can be fixed by the user. The program then gives the cheapest combination among those that have an $LPSP$ value inferior to $LPSP_{\max}$. Design of systems able to fulfill the whole need ($LPSP_{\max} = 0\%$) was target in the validation process. But the necessity of using a system having the possibility to fulfill the whole need remains questionable. Figure 2.12 helps to answer this question. Considering the house s' PV battery system, the program proposed the best solution for different value of $LPSP_{\max}$. One can see that for $LPSP_{\max}$ equal to 10%, the design system is 16% cheaper than the one of $LPSP_{\max}$ equal to 0%. In addition, this latter has only 4 hours where the whole yearly need is not fulfilled. The same study performed for the health care center gave a system 20% cheaper than the one found for a $LPSP_{\max}$ of 0%. This, with only 26 hours where the whole need is not fulfilled. Even if the solutions found with an $LPSP_{\max}$ of 0% are the most feasible, those with a $LPSP_{\max}$ of 10% are clearly more convenient.

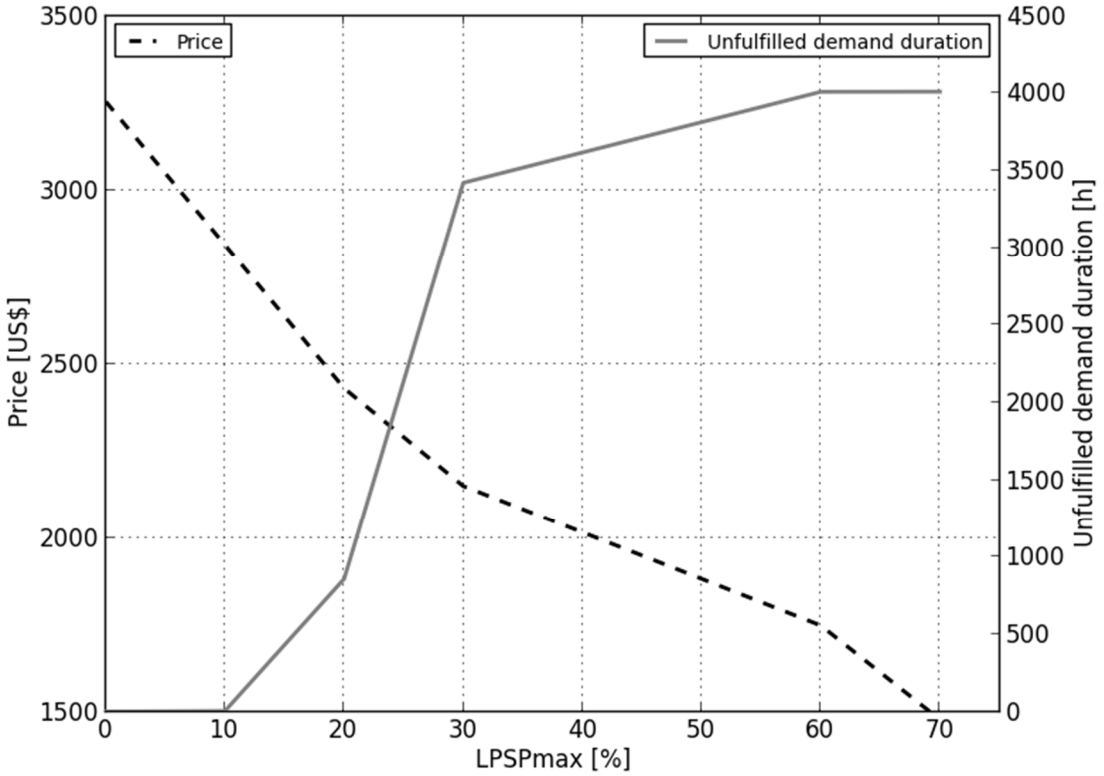

Figure 0.12 : Price and Unfulfilled demand duration of the house's PV battery system for different values of $LPSP_{\max}$

The expected period of lack of power and its probability to happen must be indicated to the population so that they can adapt their selves. Lower value of $LPSP_{\max}$ allows having cheaper system. As showed in Figure 2.12, a system with probability of loss of power supply of 20%, 30%, 60%, or 70% will be respectively 25%, 33%, 46% and 54% cheaper than the one designed to fulfill the whole needs.

2.5.6 Comparison with other technology

The main purpose of this study is to design cost effective energetic system that can supply the electricity need of remote communities. Decentralised electrification by the means of PV battery systems is used. To emphasize the asset of this technology, a comparison with the grid

extension and diesel generator was performed. To get closer to reality, ten houses are considered instead of the one previously considered. Thus, the energy need of the PV battery systems is 4699 kWh. The corresponding total net present value is 40642US$. The World Bank estimates the electricity consumption per habitant in Kenya at 167 kWh [27], thus based on this approximation, the community is constituted by 29 members.

2.5.6.1 Grid extension

Extending the grid can be a more cost-effective solution than the PV battery systems depending on the remoteness of the community and the energy demand. The break-even grid extension distance is given by the following equation:

$$NPV = (C_{cap,grid} + C_{OM,grid}) * D_{grid} + (C_{power,grid} + \mathrm{C}_{distribution}) * E_{demand} \quad (2.46)$$

Where:

$C_{cap,grid}$: capital cost of grid extension [US$/km]

$C_{OM,grid}$: O&M cost of grid extension [US$/y/km]

D_{grid} : break even grid extension distance [km]

$C_{power,grid}$: cost of power from the grid [US$/kWh]

$\mathrm{C}_{distribution}$: distribution charge [US$/kWh]

E_{demand} : total annual electricity demand [kWh/y]

NPV : total Net Present Value of the PV battery systems

In Kenya, the capital cost of grid extension is estimated at 157470 US$/km [28] the cost of power from the grid is at 0.17 US$/kWh in 2018 [28] and the distribution charge at 0.1027 US$/kWh [28]. The O&M cost is fixed at 1% of the capital cost.

Using this model, a breakeven distance of 247 m was obtained. Meaning that, even if the grid was only 247 m far from the community, the designed PV battery systems will still be most cost effective. This result is not astonishing given the small energy demand. In fact for a demand 10 times greeter i.e. a population of 390 members, the breakeven distance become almost 2.5 km. And for a big community of 3900 members, an extension of a grid 20 km far from the area will be cheaper than using PV battery system. Thus, even if PV battery systems are the presently best solutions, the future growth of the population might lead to a grid extension. However, the decrease of PV modules and batteries price can keep the PV battery technology cheaper.

2.5.6.2 Diesel generator

Even with the drop of PV modules and battery price, diesel generator is still used for electrification of remote areas. A comparison of these two technologies is performed for the whole lifetime project. The diesel generator is modelled by the following equation:

$$C_{gen,totale} = \sum_{j=1}^{N_{rep}} C_{generator} + C_{total,fuel} \tag{2.47}$$

$$C_{total,fuel} = T * C_{fuel} * (0.246 * P_{gen,nom} + 0.08415 * \sum_{i=0}^{8760} P_{load}) \tag{2.48}$$

with:

$C_{gen,totale}$: total cost of the generator use [US$]

$C_{generator}$: price of the generator [US$]

C_{fuel} : fuel price [US$]

$P_{gen,nom}$: generator nominal power [kW]

P_{load} : power demand for an hour

N_{rep} : number of replacements of the generator

T: project lifetime

The fuel price is estimated at 0.99US$/l in Kenya [29]. An NTC 3.5 kVA diesel genset which costs 1146US$ was chosen. The project lifetime is fixed at 20 years. Generator is planned to be change after 10 years.

A total cost of 66049 US$ is obtained for 20 years of operation. It is 38% more expensive than the PV battery systems. This is explained by the fact the fuel must be bought during the whole project lifetime. In fact, the expense on fuel represents 96% of the total cost. It confirms that despite their relatively high initial cost, PV battery systems are more cost effective than diesel genset in lifetime project perspective. In addition, 64401 liter of diesel is consumed during the twenty years of operation which corresponds to 173.8 tonne of CO_2 [30]. This represents a second asset of using PV battery systems instead of diesel generator.

2.6 Conclusion

Almost 1 billion people in the world are in need of water and electricity. Policies adapted by some rulers are sometimes not adapted and can end into failure. The consequences can be disastrous: increasingly harsh living conditions in rural areas, encouraging a rural exodus which weakens rural areas and increases the demand for electricity in urban centers with the development of shantytowns in cities, failing of all governmental actions in the fields of education, health, entrepreneurship and finally the increase of the insecurity. On the other hand, most parts of these countries have a very good solar potential. These make the use of decentralised PV-battery systems highly suitable.

Unfortunately, most of the softwares and programs used for PV system design remain non-affordable for these people. Hence, a free access program using an innovation design process was meant to be created to ensure accurate and precise modelling of the different components of the systems. It allows price optimization and enhancements of the included database.

A coarse sizing process is firstly used to define the maximum sizes of the different components of the system. A precise modelling of each component that enables the simulation of the behaviour of the system is then completed. Different configurations are tested during the simulation and the one fitting the best to the feasibility and cost effectiveness condition is chosen as the optimal solution. Genetic Algorithm being used as a mean to find the optimal choice in a shorter period of time. To validate the result of the program, HOMER and iHOGA were used as references. A difference in the energy calculation was brought to light. These calculation differences due to the modelling was found to be very weak for iHOGA (<2%) and significant for HOMER (>10%). Despite these calculation differences, the solution found by the three programs was found to be similar. Thus the program was found to be suitable for the optimal sizing of PV battery systems.

A discussion on the LPSPmax value was also performed. Designing a system that probably fulfills the whole electricity need was not found to be convenient. In fact lower values of LPSPmax allow having cheaper system that fulfilled a large portion of the demand. Thus, the program, by allowing the LPSPmax value being fixed by the user, makes sure that a solution adapted to the household purchasing power is found.

Then comparisons with a grid extension and diesel genset were performed. It revealed that in our case, the PV battery systems are by far most cost effective. The diesel genset was found to be 38% more expensive and reaching 173.8 tone of CO_2 for 20 years.

2.7 List of bibliographic references

[1] IEA, Energy Access Outlook, 2017, Available from: https://www.iea.org/publications/freepublications/publication/WEO2017SpecialReport_EnergyAccessOutlook.pdf

[2] Kende-Robb, "Lights, Power, Action": Electrifying Africa , African Development Bank Group, Africa progress panel , available from: http://www.africaprogresspanel.org/wp-content/uploads/2017/04/APP_Lights_Power_Action_Web_PDF_Final.pdf, 2015.

[3] Moner-Girona M., S.Szabo, S.Bhattacharyya, Off-grid photovoltaics technologies in the Solar Belt: Finance Mechanisms and incentives, 2016

[4] Eltamaly M. A., Mohamed M. A., A novel software design and optimization of hybrid power systems, the Brazilian Society of Mechanical Sciences and Engineering, 2015

[5] Kaldellis J. K., Optimum techno economic energy autonomous photovoltaic solution for remote consumers throughout Greece, Energy Conversion and Management, vol. 45, no. 17, pp. 2745-2760, 2004

[6] El-Hefnawi S. H., Photovoltaic diesel-generator hybrid power system sizing, Renewable Energy

[7] Khatib and al. developed tool for an optimal sizing of PV system in Malaysia

[8] TRNSYS, TRNSYS 17 a TRaNsient System Simulation program; Available from: http://web.mit.edu/parmstr/Public/TRNSYS/04-MathematicalReference.pdf, 2009.

[9] Green H. J., Manwell J., HYBRID2- A versatile model of the performance of hybrid power systems, Proceedings of WindPower'95, Washington DC. 27-30 March 1995

[10] HOMER ENERGY, HOMER pro version 3.7 user manual, August 2016; Available from: http://www.homerenergy.com/pdf/HOMERHelpManual.pdf

[11] HOGA, iHOGA version 2.3 user's manual, 2017, Available from: http://personal.unizar.es/rdufo/iHOGA%202.3%20User%20manual-web.pdf

[12] Barley C. D., Winn C. B., Flowers L., Green H. J., Optimal control of remote hybrid power systems, Part I: simplified model, Proceedings of WindPower'95. Washington DC, 27-30 March 1995

[13] Dufo-Lòpez R., Bernal-Augustìn J. L., Design and Control strategies of PV-Diesel systems using genetic algorithms, Solar Energy, 2004 Energy, vol. 13, no. 1, pp. 33-40, 1998

[14] Mark H., Stand-Alone Solar Electric Systems: The Earthcan Expert Handbook for Planning, Design and Installation, EARTHSCAN EXPERT SERIES, 2014

[15] Labouret A., Villoz M., ÉNERGIE SOLAIRE PHOTOVOLTAIQUE, Environnement et Sécurité : LE MONITEUR, 2009

[16] Duffie J. A. and Beckman W. A., Solar Engineering of Thermal Processes, Solar Energy Laboratory University of Wiscinsin-Madison, WILEY

[17] Liu Benjamin, Jordan Richard, A rational procedure for predicting the long term average performance of flat plate solar energy collectors, Solar Energy, 1963.

[18] Erbs, D. G., S. A. Klein, and J. A. Duffie, Estimation of the Diffuse Radiation Fraction for Hourly, Daily and Monthly Average Global Radiation, Solar Energy, 28, 293 (1982).

[19] King D.L., Boyson W.E. and Kratochvill J.A., Photovoltaic Array Performance Model, SANDIA Report, 2004

[20] Coppeti J. B., Lorenzo E., Chenlo F., A general battery model for PV system simulation, Solar Energy, 1993.

[21] King D. l., Gonzalez S., Galbraith G. M. and Boyson W. E., Performance for Grid-Connected Photovoltaic Inverters, SANDIA REPORT, September 2007.

[22] Yildizoglu Murat, Vallée Thomas, Présentation des algorithms geénétiques et de leurs applications en économies, 2004

[23] Laurent Chéno, Bibliothèque pour python

[24] Hay, J. E. and J. A. Davies, Calculation of the Solar Radiation Incident on an Inclined Surface, in Proceedings of the First Canadian Solar Radiation Data Workshop (J.E. Hay and T. K. Won, eds.), Ministry of Supply and Services, Toronto, Canada, p. 59 (1980).

[25] Manwell J. F., McGowan J. G., Lead Acid battery Storage Model for Hybrid energy systems, Solar Energy, 1993.

[26] WHOLESALE SOLAR; Availaible from https://www.wholesalesolar.com/deep-cycle-solar-batteries

[27] The World Bank, Electric power consumption (kWh per capita), 2014.

[28] Zeyringer Marianne, Pashauri Shonali, Schmid Erwin, Schmidt Johannes, Worell Ernst, Morawetz Ulrich, Analysing grid extension and stand-alone photovoltaic systems for the cost-effective electrification of Kenya, Energy for Sustainable Development, 2015

[29] Kenya Diesel price, liter, GlobalPetrolPrices.com available from: https://www.globalpetrolprices.com/Kenya/diesel_prices/

[30] Jakhrani Abdul Qayoom, Rigit Andrew Ragai Henry , Othman Al-Khalid , Samo Saleem Raza , Kamboh Shakeel Ahmed, Estimation of carbon footprints from diesel generator estimation, IEEE, 2012

CONCLUSION

Almost 1 billion people in the world are in need of water and electricity. Policies adapted by some rulers are sometimes not adapted and can end into failure. The consequences can be disastrous: increasingly harsh living conditions in rural areas encouraging a rural exodus which weaken rural areas and increase the demand for electricity in urban centers with the development of shantytowns in cities, failing of all governmental actions in the fields of education, health, entrepreneurship and finally the increase of the insecurity. On the other hand, most part of these countries has a very good solar potential. These make the use of decentralised PV-battery system suitable in these countries.
Unfortunately, most softwares and programs used for PV systems design remain non-affordable for these people.

Hence, a free access program using an innovative design process was formulated to ensure accurate and precise modelling of the different components of the systems. It allows price optimization and enhancements of the included database.

1. A coarse sizing process is first used to define the maximum sizes of the different components of the system. A precise modelling of each component that enables the simulation of the behaviour of the system is then completed. Different configurations are tested during the simulation and the one fitting the best to the feasibility and cost effectiveness condition is chosen as the optimal solution. Genetic Algorithm being used as a mean to find the optimal choice in a shorter period of time. To validate the result of the program, HOMER and iHOGA were used as references. A difference in the energy calculation was brought to light. These calculation differences due to the modelling was found to be very weak for iHOGA (<2%) and significant for HOMER (>10%). Despite these calculation differences, the solution found by the three programs was found to be similar. Thus the program was found to be suitable for the optimal sizing of PV battery systems.

A discussion on the LPSPmax value was also performed. Designing a system that probably fulfills the whole electricity need was not found to be convenient. In fact, lower values of LPSPmax allow having cheaper system that fulfilled a large portion of the demand. Thus, the program, by allowing the LPSPmax value being fixed by the user, makes sure that a solution adapted to the household purchasing power is found.

Then comparisons with a grid extension and diesel genset were performed. It revealed that in our case, the PV battery systems are by far most cost effective. The diesel genset was found to be 38% more expensive and reaching 173.8 tone of CO_2 for 20 years.

ANNEX I

LOAD DEMAND'S PAPER SHEETS: THE CASE OF ELDORET

Table A I-1: Lamps and Applicances

	Appareil	Puissance	Voltage	Debut1	Fin1	Debut2	fin2	DC/AC
Maison	Lampe LED	18	12	19	23	6	7	1
Eclair. Pub	LampeFluor	60	12	19	23	6	7	1
	Sitting Room	30	12	19	23	6	7	1
	water pump	40	12	6	7	0	0	1
	TV	80	240	19	22	0	0	-1
	Music player	15	240	19	22	0	0	-1
	Laptop	25	240	20	22	0	0	-1
	10lampadaires	18	12	19	23	0	7	1
Poste de santé	1 lampe	10	12	19	23	5	7	1
	2 lampes	10	12	19	23	6	7	1
	1 ventilateur	60	12	12	16	0	0	1
	1 radio	40	12	6	7	19	20	1
	1 réfregat	70	12	0	23	0	0	1
École	2 lampes	10	12	17	19	0	0	1
	1 télévision	80	240	10	11	0	0	-1
	1 ordinateur-Laptop	100	240	9	11	15	17	-1
	1 imprimante	50	240	11	12	0	0	-1

ANNEX II

DATABASE OF DIFFERENT COMPONENT OF PV-BATTERY SYSTEM: THE CASE OF ELDORET

Table A II-1: PV modules ' specifications

Name	Isc	Voc	Imp	Vmp	Pmax	muV	muI	NOTC	Price
SLP100-12U_Poly	6,46	21,6	5,81	17,2	100	-0,08	0,00065	47	224,75
SLP120-24U_Poly	3,86	43,2	3,49	34,4	120	-0,08	0,00065	47	269,7
SLP120-12U_Poly	7,72	21,6	6,98	12,2	120	-0,08	0,00065	47	269,7
SLP09012M_Poly	5,81	21,6	5,23	17,2	90	-0,08	0,00065	47	208,8
SLP160S12_Mono	9,6	21,9	8,8	18,2	160	-0,08	0,00065	47	324,8
SLP070-12M_Poly	4,51	21,6	4,07	12,2	70	-0,08	0,00065	47	177,63
SLP45-12U_Poly	2,92	21,6	2,62	17,2	45	-0,08	0,00065	47	123,98
SLP030-24U_Poly	0,96	43,2	0,87	34,4	30	-0,08	0,00065	47	91,28
SLP015-06_Poly	0,67	10,5	0,58	8,6	15	-0,08	0,00065	47	52,2
SLP015-12U_Poly	0,96	21,6	0,87	12,2	15	-0,08	0,00065	47	52,2
SLP010-12U_Poly	0,68	21,6	0,58	17	10	-0,08	0,00065	47	35,53
SLP005-12U_Poly	0,34	21,6	0,29	17	5	-0,08	0,00065	47	22,84

Table A II-2: PV modules ' specifications

Name	Voltage	Efficiency
SLP100-12U_Poly	12	0,15
SLP120-24U_Poly	24	0,15
SLP120-12U_Poly	12	0,15
SLP09012M_Poly	12	0,15
SLP160S12_Mono	12	0,15
SLP070-12M_Poly	12	0,15
SLP45-12U_Poly	12	0,15
SLP030-24U_Poly	24	0,15
SLP015-06_Poly	6	0,15
SLP015-12U_Poly	12	0,15
SLP010-12U_Poly	12	0,15
SLP005-12U_Poly	12	0,15

Table A II-3: Batteries ' specifications

Name	Type	Capacity	Discharge Time	Price	Voltage
Crown 12CRV110	Absorbant Glass Mat	110	20	235	12
Crown 6CRV220	Absorbant Glass Mat	220	20	229	6
Fullriver DC105 12AGM	Absorbant Glass Mat	105	20	245	12
Fullriver DC160 12AGM	Absorbant Glass Mat	160	20	365	12
Fullriver DC210 12AGM	Absorbant Glass Mat	210	20	485	12
Fullriver DC224 6AGM	Absorbant Glass Mat	224	20	239	6
UPG UB12500 AGM	Absorbant Glass Mat	90	20	103	12
UPG UB12900 AGM	Absorbant Glass Mat	90	20	177	12
UPG UB-121000 AGM	Absorbant Glass Mat	100	20	187	12
Crown 6CRV390	Absorbant Glass Mat	390	20	471	6
Surrette / Rolls S-550	FloodedLead Acid	428	20	365	6

Table A II-4: Batteries ' specifications

Name	Self Discharge	Charging efficiency	Discharging efficiency
Crown 12CRV110	0,02	0,9	1
Crown 6CRV220	0,02	0,9	1
Fullriver DC105 12AGM	0,02	0,9	1
Fullriver DC160 12AGM	0,02	0,9	1
Fullriver DC210 12AGM	0,02	0,9	1
Fullriver DC224 6AGM	0,02	0,9	1
UPG UB12500 AGM	0,02	0,9	1
UPG UB12900 AGM	0,02	0,9	1
UPG UB-121000 AGM	0,02	0,9	1
Crown 6CRV390	0,02	0,9	1
Surrette / Rolls S-550	0,02	0,9	1

Table A II-5: Inverters' specifications

Name	Pnom	Effciciency	Vdc	Vac	Price
Cotek S150 112	150	87	12	120	149
Cotek S300 112	300	87	12	120	163
Cotek S600 112	600	87	12	120	299
Cotek S1500 112	1500	87	12	120	499
Cotek S150 124	150	87	24	120	149
Cotek S300 124	300	87	24	120	163
Cotek S600 124	600	87	24	120	299
Cotek S1500 124	1500	87	24	120	499

APPENDIX A

SANDIA'S PV MODULE MODELLING

The calculations are performed with the following equations:

$$I_{sc} = I_{sc_0}.f_1(AM_a).[(\mathrm{E}_b.f_2(AOI) + f_d.E_{diff})/E_0].[1+\alpha_{I_{sc}}.(T_c - T_0)] \quad \text{(A A-1)}$$

$$I_{mp} = I_{mp0}.[C_0.E_e + C_1.E_e^2].[1+\alpha_{1_{mp}}.(T_c - T_0)] \quad \text{(A A-2)}$$

$$V_{oc} = V_{oc_0} + N_s.\delta(T_c).\ln(E_e) + \beta_{V_{oc}}(E_e).(T_c - T_0) \quad \text{(A A-3)}$$

$$V_{mp} = V_{mp0} + C_2.N_s.\delta(T_c).\ln(E_e) + C_3.N_s.[\delta(T_c).\ln(E_e)]^2 + \beta_{V_{mp}}(E_e).(T_c - T_0) \quad \text{(A A-4)}$$

$$P_{mp} = I_{mp}.V_{mp} \quad \text{(A A-5)}$$

$$FF = P_{mp}/(I_{sc}V_{oc}) \quad \text{(A A-6)}$$

with E_e the effective solar irradiance and $\delta(T_c)$ the thermal voltage given by:

$$E_e = I_{sc}/[I_{sc_0}.[1+\alpha_{I_{sc}}.(T_c - T_0)]] \quad \text{(A A-7)}$$

$$\delta(T_c) = n.k.(T_c + 273.15)/q \quad \text{(A A-8)}$$

$$I_x = I_{x0}.[\mathrm{C}_4.E_e + C_5.E_e^2].[1+\alpha_{I_{sc}}.(T_c - T_0)] \quad \text{(A A-9)}$$

$$I_{xx} = I_{xx0}.[C_6.E_e + C_7.E_e^2].[1+\alpha_{I_{mp}}.(T_c - T_0)] \quad \text{(A A-10)}$$

$$C_0 + C_1 = 1 \quad \text{(A A-11)}$$

$$C_4 + C_5 = 1 \quad \text{(A A.12)}$$

$$C_6 + C_7 = 1 \quad \text{(A A-13)}$$

APPENDIX B

RESOLUTION OF THE KIBAM's MODEL

For mathematical simplicity a new rate constant k was defined as:

$$k = \frac{k'}{c(1-c)} \tag{A B-1}$$

Regarding the equation 1.69, three constants are to be determined to explicitly define q_1 : the initial amount of charge $q_{1,0}$, c and k. In this purpose, the ratio F_t is defined as:

$$F_t = F_{t_1,t_2} = \frac{q_{T=t_1}}{q_{T=t_2}} = \frac{t_1}{t_2}\left[\frac{(1-e^{-kt_2})(1-c)+kct_2}{(1-e^{-kt_1})(1-c)+kct_1}\right] \tag{A B-2}$$

where $q_{T=t}$ the discharge capacity at discharge time $T = t$

The previous equation can be written:

$$c = \frac{F_t(1-e^{-kt_1})t_2 - (1-e^{-kt_2})t_1}{F_t(1-e^{-kt_1})t_2 - (1-e^{-kt_2})t_1} - kF_t t_1 t_2 + kt_1 t_2 \tag{A B-3}$$

If for two different values of F_{t_1,t_2} same values of c and k are found, this latter c and k values are the one to be used.

Manwell and al. proposed to find the maximum capacity of the battery q_{max} by using reasonably slow discharge rate, such as 20-h rate. It gives:

$$q_{\max} = \frac{q_{T=20}[(1-e^{-k20})(1-c)+kc20]}{kc20} \qquad \text{(A B-4)}$$

LIST OF BIBLIOGRAPHICAL REFERENCES

Achaibou N., Haddadi M., Malek A., Modeling of lead acid batteries in PV systems, Energy Procedia 18 538 – 544, 2012.

Ameen A. M., Pasupuleti J. and Khatib T., Simplified performance models of photovoltaic/diesel generator/battery system considering typical control strategies, Energy Conversion and Management, 2015.

Barley C. D., Winn C. B., Flowers L., Green H. J., Optimal control of remote hybrid power systems, Part I: simplified model, Proceedings of WindPower'95. Washington DC, 27-30 March 1995

Collares-Pereira, M. and A. Rabl, The Average Distribution of Solar Radiation Correlations Between Diffuse and Hemispherical and Between Daily and Hourly Insolation Values, Solar Energy, 22, 155 (1979a).

Coppeti J. B., Lorenzo E., Chenlo F., A general battery model for PV system simulation, Solar Energy, 1993.

Duffie J. A. and Beckman W. A., Solar Engineering of Thermal Processes, Solar Energy Laboratory University of Wiscinsin-Madison, WILEY

Dufo-Lòpez R., Bernal-Augustìn J. L., Design and Control strategies of PV-Diesel systems using genetic algorithms, Solar Energy, 2004

El-Hefnawi S. H., Photovoltaic diesel-generator hybrid power system sizing, Renewable Energy, vol. 13, no. 1, pp. 33-40, 1998

Eltamaly M. A., Mohamed M. A., A novel software design and optimization of hybrid power systems, the Brazilian Society of Mechanical Sciences and Engineering, 2015

Erbs, D. G., S. A. Klein, and J. A. Duffie, Estimation of the Diffuse Radiation Fraction for Hourly, Daily and Monthly Average Global Radiation, Solar Energy, 28, 293 (1982).

France Lasnier and Tony Gan, Photovoltaic engineering handbook, Bristol 1990

Geetha, R. and Srikanth U.G., Ant colony optimization in different engineering applications: An overview, Journal of Computer Applications, 49: 19-25. DOI: 10.5120/7720-1091, 2012.

Green H. J., Manwell J., HYBRID2- A versatile model of the performance of hybrid power

systems, Proceedings of WindPower'95, Washington DC. 27-30 March 1995

Guasch D. and Silvestre S., Dynamic Battery Model for Photovoltaic Applications, PROGRESS IN PHOTOVOLTAICS: RESEARCH AND APPLICATIONS, 2003.

Hansen, N., Ros R., Mauny N., Schoenauer M. and Auger A. PSO facing non-separable and ill-conditioned problems, Universite Paris, , 2008.

Hay, J. E. and J. A. Davies, Calculation of the Solar Radiation Incident on an Inclined Surface, in Proceedings of the First Canadian Solar Radiation Data Workshop (J.E. Hay and T. K. Won, eds.), Ministry of Supply and Services, Toronto, Canada, p. 59 (1980).

Hybrid2, The Hybrid System simulation model Version 1.0 user manual, 1996, Available from: https://www.nrel.gov/docs/legosti/old/21272.pdf

HOMER ENERGY , HOMER pro version 3.7 user manual, August 2016; Available from: http://www.homerenergy.com/pdf/HOMERHelpManual.pdf

Hottel, H. C., A Simple Model for Estimating the Transmittance of Direct Solar Radiation Through Clear Atmospheres, Solar Energy,18, 129 (1976).

HOGA, iHOGA version 2.3 user's manual, 2017, Available from: http://personal.unizar.es/rdufo/iHOGA%202.3%20User%20manual-web.pdf

IRENA, RENEWABLE ENERGY STATISTICS 2017, 2017

Kaldellis J. K., Optimum techno economic energy autonomous photovoltaic solution for remote consumers throughout Greece, Energy Conversion and Management, vol. 45, no. 17, pp. 2745-2760, 2004

Kende-Robb, "Lights, Power, Action": Electrifying Africa , African Development Bank Group, Africa progress panel , available from: http://www.africaprogresspanel.org/wp-content/uploads/2017/04/APP_Lights_Power_Action_Web_PDF_Final.pdf, 2015.

Khatib and al. developed tool for an optimal sizing of PV system in Malaysia

King D.L., Boyson W.E. and Kratochvill J.A., Photovoltaic Array Performance Model, SANDIA REPORT, 2004

King D. l., Gonzalez S., Galbraith G. M. and Boyson W. E., Performance for Grid-Connected Photovoltaic Inverters, SANDIA REPORT, September 2007.

Konrad Mertens, Photovoltaics: Fundamentals, Technology and Practice, WILEY, 2014

Kreith F., J. F. Kreider, Principles of solar engineering, Hemisphere Pub Corp, 1978,

Labouret A., Villoz M., ÉNERGIE SOLAIRE PHOTOVOLTAIQUE, Environnement et Sécurité : LE MONITEUR, 2009

Liu, B. Y. H. and R. C. Jordan, The Interrelationship and Characteristic Distribution of Direct, Diffuse and Total Solar Radiation, Solar Energy, 4 (3), 1 (1960).

Loutzenhiser P.G., Empirical validation of models to compute solar irradiance on inclined surfaces for building energy simulation, Solar Energy vol. 81. pp. 254-267, 2007.

Manwell J. F., McGowan J. G., Lead Acid battery Storage Model for Hybrid energy systems, Solar Energy, 1993.

Mark H., Stand-Alone Solar Electric Systems: The Earthcan Expert Handbook for Planning, Design and Installation, EARTHSCAN EXPERT SERIES, 2014

Moner-Girona M., S.Szabo, S.Bhattacharyya, Off-grid photovoltaics technologies in the Solar Belt: Finance Mechanisms and incentives, 2016

Reindl, D. T., M. S., Estimating Diffuse Radiation on Horizontal Surfaces and Total Radiation on Tilted Surfaces, Thesis, Mechanical Engineering, University of Wisconsin-Madison (1988).

Retscreen, Retscreen software online user manual, Clean Energy Support Center; Availablefrom: http://www.mcit.gov.cy/mcit/mcit.nsf/0/EF620C37922EDAECC22575CB00457F21/$file/Retscreen%20Manual%20(CHP).pdf

Saishanmuga, V.R. and Rajagopalan S.P., A neuro-genetic system for face recognition, Journal of Computer Science, India, 2012.

Saishanmuga V. R. and Rajagopalan S.P., A comparative analysis of optimization technics of Artificial Neutral Network in Biomedical Applications, Journal of computer science, India, 2013

Shaw P., Sahu P. K., Maity S. and Kumar P., Modelling and Control of a battery connected standalone photovoltaic system, IEEE, 2017.

Shukla K. N., S. Rangnekar, K.Sudhakar, Comparative study of isotropic and anisotropic sky

models to estimate solar radiation incident on tilted surface: A case study of Bhopal India, Energy Reports, 2015.

Tan K. T., So P. L., Chu Y. C. and Kwan K. H., Modeling, Control and Simulation of a Photovoltaic Power System for Grid-connected and Stand-alone Applications, IEEE, 2010

TRNSYS, TRNSYS 17 a TRaNsient System Simulation program; Available from: http://web.mit.edu/parmstr/Public/TRNSYS/04-MathematicalReference.pdf, 2009.

Xu D., Kang L., Chang L. and Cao B., Optimal Sizing of standalone hybrid wind/PV power systems using genetic algorithms, IEEE ,2005